Routing a Mix of Conventional, Plug-in Hybrid, and Electric Vehicles

Gerhard Hiermann, Richard F Hartl, Jakob Puchinger, Thibaut Vidal

Routing a Mix of Conventional, Plug-in Hybrid, and Electric Vehicles

Gerhard Hiermann[a,*], Richard F. Hartl[b], Jakob Puchinger[c,d], Thibaut Vidal[e]

[a] *nuwings OG, Austria*
[b] *Department of Business Administration, University of Vienna, Austria*
[c] *Laboratoire Genie Industriel, CentraleSupélec, Université Paris-Saclay, France*
[d] *Institut de Recherche Technologique SystemX, Palaiseau, France*
[e] *PUC-Rio, Pontifical Catholic University of Rio de Janeiro, Brazil*

Abstract

We introduce an electric vehicle routing problem combining conventional, plug-in hybrid, and electric vehicles. Electric vehicles are constrained in their service range by their battery capacity, and may require time-consuming recharging operations at some specific locations. Plug-in hybrid vehicles have two engines, an internal combustion engine and an electric engine using a built-in rechargeable battery. These vehicles can avoid visits to recharging stations by switching to fossil fuel. However, this flexibility comes at the price of a generally higher consumption rate and utility cost.

To solve this complex problem variant, we design a sophisticated metaheuristic which combines a genetic algorithm with local and large neighborhood search. All route evaluations, within the approach, are based on a layered optimization algorithm which combines labeling techniques and greedy evaluation policies to optimally insert recharging stations visits in a fixed trip and to select the fuel types. The metaheuristic is finally hybridized with an integer programming solver, over a set partitioning formulation, so as to recombine high-quality routes from the past search into better solutions. Extensive experimental analyses are conducted, highlighting the good performance of the algorithm and the contribution of each of its main components.

Finally, we investigate the impact of fuel and energy cost on fleet composition decisions. Our experiments show that a careful use of a mixed fleet can significantly reduce operational costs in a large variety of price scenarios, in comparison with the use of a fleet composed of a single vehicle class.

Keywords: Routing, Electric Vehicles, Plug-In Hybrid, Heterogeneous Fleets, Hybrid Metaheuristics

1. Introduction

Climate change is a major concern for humankind, and it is essential to reduce anthropogenic greenhouse gas emissions. Major emission sources are energy production, industry, agriculture, and transportation. Governmental institutions all over the world seek to reduce the emission of carbon-dioxide equivalents by introducing new regulations (Edenhofer et al., 2014). This has led to increased research into more efficient and cleaner ways to use fossil fuel as well as alternative types of engines. In recent years, the production of battery electric vehicles (BEVs) for large markets has increased, and considerable efforts have been made to reduce vehicle and battery costs (AustriaTech, 2014). However, the relatively limited capacity of batteries considerably reduces the operational range of BEVs, such that time-consuming visits to recharging stations must be considered in the planning phase.

Hybrids vehicles with features of both BEVs and internal combustion engine vehicles (ICEVs) have been developed to reduce the necessary stops and the infrastructure dependence. The so-called plug-in hybrid electric vehicles (PHEVs) have two engines—an internal combustion engine (ICE) and a pure electric engine—that can be easily switched, permitting the use of electric mode on selected route segments. PHEVs

*Corresponding author
Email addresses: gerhard.hiermann@nuwings.at (Gerhard Hiermann), richard.hartl@univie.ac.at (Richard F. Hartl), jakob.puchinger@centralesupelec.fr (Jakob Puchinger), vidalt@inf.puc-rio.br (Thibaut Vidal)

do not have the operational range restriction of BEVs, and they can recharge en route to reduce the use of fossil fuel on other trip segments, which can be beneficial in terms of cost and emissions. However, two engines also means a heavier base load, which in turn leads to a higher consumption of both electricity and fuel. Each technology has its merits, and with the variety of subtypes available (AustriaTech, 2014), choosing the best fleet mix for a given transport demand is a very difficult task.

In this article, we introduce a hybrid heterogeneous electric fleet routing problem with time windows and recharging stations (H^2E-FTW). This problem considers three different vehicle classes—ICEV, BEV, and PHEV—as well as multiple vehicle types for each class, differing in capacity, battery size, and electric energy and/or fuel consumption per mile. The batteries of BEVs and PHEVs can be charged at recharging stations. To retain a simple problem formulation and focus on the fleet-composition decisions, we assume that the recharging time is proportional to the amount of energy charged. For PHEVs, the engine type used can be switched at any given time by the driver or an on-board unit. The routing cost consists of the electric energy and the fuel consumption weighted by their respective costs. The number of vehicle classes and types used in the final mix is not limited, but a fixed cost per usage balances the fleet cost with the consumption-based variable cost. By integrating tour planning and vehicle selection within this problem, we aim to achieve better overall plans compared to those obtained by sequential decisions. To this date, integrated approaches have not been often considered in the literature, especially for ICEVs, BEVs, and PHEVs of different types.

The three vehicle classes differ in the need to recharge and to choose the engine. To account for these decisions, we propose a systematic route evaluation approach using decision layers, hence progressing towards a unified view of the problem. These layers separate the vehicle-specific knowledge from the higher-level solution procedure, and this generic design allows us to apply either existing or new metaheuristic approaches and operators. Based on the characteristics of the problem, the vehicle routing problem with time windows (VRPTW) is viewed as the highest unifying layer. In the lower layers of the algorithm, we use labeling algorithms for the placement of recharging stations and greedy policies for the engine use. Finally, we rely on an efficient hybrid genetic algorithm (HGA) with a local search (LS) for solution intensification, along with state-of-the-art population management techniques for diversification. Two additional components are also included: a set partitioning component, which is regularly used to create a new solution based on routes discovered in the past search; and a large neighborhood search (LNS) which acts as a mutation operator.

Through extensive numerical studies, we evaluate the performance of this metaheuristic on a variety of benchmark instances and problem variants. For the special case of the heterogeneous fleet size and mix problem considering only BEVs (E-FSMFTW; Hiermann et al., 2016; Montoya, 2016), our approach finds solutions of better quality than previous algorithms in a similar time. Additional comparative analyses, on the electric VRPTW with recharging stations (E-VRPTW; Schneider et al., 2014) and partial recharging (E-VRPTWPR; Keskin & Çatay, 2016) further demonstrate the competitiveness of our approach. Finally, to gain additional managerial insights, we performed sensitivity analysis to evaluate the merits of a mixed vehicle fleet, and measure the impact of fuel and electricity costs on fleet composition. The main contributions of this work are:

- the definition of an integrated routing and vehicle selection problem with ICEVs, PHEVs, and BEVs;
- a sophisticated solution algorithm, based on a new systematic search method using multiple decision layers for route evaluation;
- an extension of the metaheuristic with a LNS and set partitioning component;
- finally, a detailed sensitivity analysis on the impact of mixed fleet optimization and different vehicle types on operational costs, for multiple fuel and electricity cost scenarios.

2. Problem statement and literature review

In the Hybrid Heterogeneous Electric Fleet routing problem with Time Windows and recharging stations (H^2E-FTW), we are given a graph $\mathcal{G}(\mathcal{V},\mathcal{E})$ and a set of vehicle types $\mathcal{K} = \mathcal{K}^I \cup \mathcal{K}^B \cup \mathcal{K}^P$, which is the union of the vehicles in the three classes: ICEV ($\mathcal{K}^I$), BEV ($\mathcal{K}^B$), and PHEV ($\mathcal{K}^P$). The set of vertices $\mathcal{V} = \{v_0, \ldots, v_{n+p}\}$ consists of a single depot v_0, a set of n customers $\mathcal{C} = \{v_1, \ldots, v_n\}$, and a set of p recharging stations $\mathcal{F} = \{v_{n+1}, \ldots, v_{n+p}\}$. Each tour starts and ends at the depot v_0, and each customer is

visited exactly once. Recharging stations are optional and can be visited by any vehicle multiple times or not at all.

A demand q_i and service time s_i is associated to each customer $v_i \in \mathcal{V}$, and each vehicle k has a capacity Q^k. For each vertex $v_i \in \mathcal{V}$, we define a service time window $[e_i, l_i]$, where e_i is the earliest and l_i the latest possible start of service. Recharging stations can be used to recharge the batteries between customer visits. Each vehicle type with a battery (i.e., BEV or PHEV) can recover a quantity of energy between the current charge level and the battery capacity Y^k, $k \in \mathcal{K}^B \cup \mathcal{K}^P$. Recharging takes a time which is assumed to be linear in the quantity of energy recharged with an inverse recharging rate g, (i.e., time = amount $\cdot\, g$). This implies that the decision on how much energy to charge is part of the routing problem. The vehicles are assumed to be fully charged when leaving the depot, and the charge level is not allowed to drop below zero.

Each vehicle k has an associated fixed cost, denoted f^k, which may represent some fraction of the acquisition, maintenance, and driver cost. The electric energy and fuel consumption rates are constants, denoted r_{E} and r_{F} respectively. Since ICEVs cannot use electricity to travel between vertices, r_{E} is defined only for $k \in \mathcal{K}^B \cup \mathcal{K}^P$. The same holds for fuel, i.e., r_{F} is defined only for $k \in \mathcal{K}^I \cup \mathcal{K}^P$. Vehicles traverse the graph using edges $(i, j) \in \mathcal{E}$, $i, j \in \mathcal{V}$, where $\mathcal{E}$ satisfies the triangle inequality. Each edge has two associated values, the distance d_{ij} and travel time t_{ij}. The electric energy and fuel consumption are linear functions of the distance and the corresponding consumption rate, i.e., $d_{ij} \cdot r_{\text{E}}$ and $d_{ij} \cdot r_{\text{F}}$ respectively. Both values can be calculated in advance for each edge and each applicable vehicle type.

PHEVs include an electric engine and an ICE. We assume that the driver can switch between them without any restrictions or penalties other than the current charge level, possibly on the way between two vertices. Finally, an electricity price c_{E} and a fuel price c_{F} is defined. These constant prices should be multiplied by the total electric energy and fuel consumed by the fleet. The objective of the H^{2}E-FTW is to minimize the sum of the fixed and variable costs.

Related work

The literature on vehicle routing problems is rich and diverse. Problems with different vehicle types are usually called heterogeneous VRPs, and are reviewed in Baldacci et al. (2008) and Toth & Vigo (2014). The research on electric vehicles has progressed on various aspects: battery technology, optimal routing, and tour planning. We refer to Pelletier et al. (2016) for a recent survey of this broad research field. We now provide a short overview of directly related work.

Conrad & Figliozzi (2011) presented one of the earliest studies of electric vehicle routing, where electric vehicles can be fast-charged to 80% of the maximum battery level at customer locations. Called the "recharging VRP", this formulation assumed a fixed charging time independent of the battery state but contributing to the objective value by imposing a recharging cost. Erdoğan & Miller-Hooks (2012) formulated a green VRP using alternative-fuel vehicles that can be refueled at dedicated stations. Electric vehicle routing and recharging stations were first considered by Schneider et al. (2014), who introduced the E-VRPTW. The benchmark set of this work was further analyzed by Desaulniers et al. (2016) using a new exact branch-and-cut-and-price algorithm. The authors define a bidirectional labeling method for full and partial recharging at single or multiple recharging stations. In parallel, Keskin & Çatay (2016) worked on a quick charging scheme that also allowed partial recharging.

Felipe et al. (2014) studied multiple recharging technologies with different costs for a single fleet type. With regards to fleet mix, Hiermann et al. (2016) extended the E-VRPTW by considering a heterogeneous fleet of BEVs. Goeke & Schneider (2015) tackled a variant of the E-VRPTW with a single type of ICEV and BEV with load-dependent energy consumption. Lebeau et al. (2015) considered multiple types of ICEVs and BEVs and proposed a small benchmark set of 21 instances, using distances from a real-world road network. However, in their formulation, recharging is possible only at the depot. A rich formulation is studied by Sassi et al. (2015). The authors consider a combined fleet and synchronization aspects of the recharging grid. A regret-based construction heuristic is initially used to solve large real-world instances.

This research focuses on the tour planning, but there have also been studies of street routing problems with electric vehicles. In particular, Zündorf (2014) provides methods to incorporate different charging technologies and presents an algorithm to determine a set of shortest energy-efficient paths. Finally, for PHEVs the literature is rather sparse, with Abdallah (2013) being one of the first to discuss a VRPTW

using a homogeneous fleet of PHEVs. The problem definition allows the vehicle to be recharged before or after serving a customer at the customer's location.

3. Methodology

The problem presented in this work is quite complex: even the evaluation of a single route (sequence of customer visits) is a hard task due to the necessity of optimizing visits to recharging stations and possible fuel changes. Based on this problem structure, we design a heuristic solution algorithm that works on solutions represented as sequences of customer visits without charging stations. During the search, and whenever a route needs to be evaluated, the method uses labeling techniques to optimally insert charging stations and greedy policies for timing, charging and mode selection decisions. Section 3.1 describes the evaluation techniques used in detail, whereas Section 3.2 shows the general search heuristic built on top of this evaluation method.

3.1. Route Evaluations Techniques

The H^2E-FTW includes three vehicle classes, and each class gives rise to a different VRP variant with different decision sets. We introduce a generic route evaluation methodology that provides a unified view of these problems and allows the use of a generic heuristic solver—in our case a genetic algorithm—working on a simple VRP representation of the problem. Therefore, the solver is decoupled from problem-specific evaluation and sequencing methods.

ICEV routing is related to the classical VRPTW (Toth & Vigo, 2014), in which no energy restrictions have to be considered. The BEVs have additional energy constraints. BEV routing is related to the E-VRPTW (Schneider et al., 2014), but with possible partial recharging, i.e., the amount of recharging is a decision variable, as in Keskin & Çatay (2016). PHEVs further extend the E-VRPTW—referred to as the PH-VRPTW in this work—by adding decisions about on the propulsion mode used. Table 3.1 summarizes the features of each subproblem.

Feature	ICEV (VRPTW)	BEV (E-VRPTW)	PHEV (PH-VRPTW)
Itinerary	x	x	x
Demand	x	x	x
Time windows	x	x	x
Energy		x	x
(Partial) recharging		x	x
Propulsion mode			x

Table 3.1: Comparison of features of each subproblem

We use a systematic evaluation framework to efficiently explore the search space. The first layer is the metaheuristic solver. It works on incomplete solutions, in which some variables are not considered. Each further layer adds more information to the solution, until a full solution, and its cost, is known in the bottom layer. Each layer uses feedback from the subsequent layer in its decision-making process, and thus the method is recursive and not sequential.

Existing solution methods implicitly use this concept, e.g., the VRPTW has two layers. In the upper layer, the assignment of customers to vehicles and the vehicles' itineraries are determined. The departure times are then implicitly determined by solving a simple *timing* subproblem (Vidal et al., 2015b). By separating problem-specific details via layers, we are able to solve the H^2E-FTW with well-studied methods from the literature. Figure 3.1 shows the layers and the corresponding decisions. The solution method at the first layer is a state-of-the-art HGA. It assigns customers to vehicles and determines the sequence of the visits. At the second layer of the E/PH-VRPTW, we solve a resource-constrained shortest path problem (RCSPP) with fixed visits using dynamic programming (DP) to determine where to insert recharging stations. The third layer determines the objective value using a greedy policy.

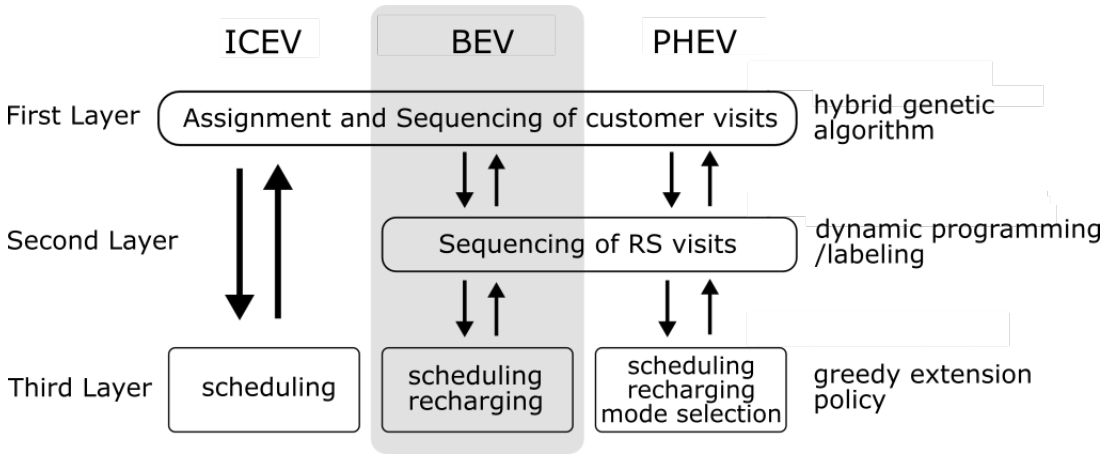

Figure 3.1: Layered representation of the H^{2}E-FTW problem.

In the following sections, the second and third layers are described in detail for both E-VRPTW and PH-VRPTW. Note that we use the term energy to refer to electric energy only.

3.1.1. Third layer – Calculation of the objective value

The third layer, as shown in Figure 3.1, works with a complete route, where all the customer and recharging-station visits are sequenced. For ICEVs, this process is already well-studied in the literature. For BEVs and PHEVs, the additional charging and mode-selection decisions are described in the following sections. We use the notation of resource extension functions (REF) to define how the value of a resource (e.g., distance) changes when a vertex is added to an already computed sequence (Irnich & Villeneuve, 2006).

Greedy charging policy (BEV)

The extension functions for the E-VRPTW with complete recharging are discussed in Hiermann et al. (2016). However, since we are considering partial recharging they had to be reformulated. The amount of recharging must be determined for every recharging station visit. Since charging operations take time, every decision has a direct impact on the feasibility of a route (e.g., the time windows might be violated). We apply a greedy recharging policy with two simple rules:

- Whenever a sequence ending in vertex i is extended by vertex j, and the electric energy required ($d_{ij} \cdot r_{\mathrm{E}}$) exceeds the current state, attempt to recharge the required amount at the last recharging station visited.
- Avoid waiting time by performing a recharging operation at the last station visited.

This policy exploits three properties of the problem:

- a vehicle needs to recharge only if it cannot complete the tour otherwise;
- electricity costs are applied to the amount consumed, not to the amount recharged;
- recharging operations can always be performed at the last recharging station visited.

The first property is straightforward: we recharge only if really necessary. The second states that the amount of energy recharged has no impact on the routing costs; this implies that waiting time can always be transformed into a charging operation. The third property exploits the linear recharging rate. A linear rate implies that all time-feasible choices of the location of the recharging operation are equivalent for all visits to recharging stations in the sequence so far, as long as they fulfill the energy capacity constraint. Therefore, using only the last one will not reduce the quality of the recharging decision.

To capture this policy in an extension function, we define the following functions to extend the data processed for a given visit sequence $\{d, \dots, i\}$ to a new visit j. The intermediate calculations, with names starting with Δ, are described in the text where they occur, and then displayed at the end of the section to simplify the descriptions.

$$T_j^{\mathrm{COST}} = T_i^{\mathrm{COST}} + d_{ij} \cdot r_{\mathrm{E}} \cdot c_{\mathrm{E}} \tag{3.1}$$

$$T_j^{\mathrm{Q}} = T_i^{\mathrm{Q}} + q_j \tag{3.2}$$

The cost and capacity resources are T_i^{COST} and T_i^{Q} respectively. An extension simply sums the cost of the consumed electric energy and additional load respectively.

$$T_j^{\mathrm{DUR}} = T_i^{\mathrm{DUR}} + t_{ij} + s_j + \Delta^{\mathrm{WT}} + \Delta^{\mathrm{T^{RC}}} \tag{3.3}$$

$$T_j^{\mathrm{TW}} = T_i^{\mathrm{TW}} + \Delta^{\mathrm{TW}} + \Delta^{\mathrm{TW^{RC}}} \tag{3.4}$$

The time resources are T_i^{DUR} for the duration of the route and T_i^{TW} for the time warp used. Using the concept of a time warp allows for a more efficient penalty scheme (Nagata et al., 2010; Vidal et al., 2015a) because time-window violations are accounted for and repaired locally and do not propagate any further. The duration is calculated by adding the travel time t_{ij}, the service time s_j, the waiting time Δ^{WT}, and the recharging time $\Delta^{\mathrm{T^{RC}}}$. The time warp T_i^{TW} is extended by adding any necessary time warp as a result of either arriving too late at the customer Δ^{TW} or a required recharging operation $\Delta^{\mathrm{TW^{RC}}}$.

$$T_j^{\mathrm{Y}} = T_i^{\mathrm{Y}} - d_{ij} \cdot r_{\mathrm{E}} + \Delta^{\mathrm{EY^{RC}}} + \Delta^{\mathrm{Y^{WT}}} \tag{3.5}$$

$$T_j^{\mathrm{EY}} = T_i^{\mathrm{EY}} + \Delta^{\mathrm{Y^{RC}}} \tag{3.6}$$

T_i^{Y} is the available electric energy of the vehicle at vertex i, whereas T_i^{EY} counts the violations due to missed recharging opportunities. T_i^{Y} is calculated by subtracting the electric energy required to reach v (i.e., $d_{ij} \cdot r_{\mathrm{E}}$) and adding any energy recharged ($\Delta^{\mathrm{EY^{RC}}}$) to avoid the violation of the energy constraint as well as the amount recharged ($\Delta^{\mathrm{Y^{WT}}}$) to avoid waiting time at the customer.

Two further resources must be processed: the amount of electricity that can be recharged T_i^{YAR} and the time available for recharging T_i^{TAR}. First,

$$T_j^{\mathrm{YAR}} = \begin{cases} Y - (T_i^{\mathrm{Y}} - d_{ij} \cdot r_{\mathrm{E}} + \Delta^{\mathrm{EY^{RC}}} + \Delta^{\mathrm{Y^{WT}}}) & \text{if } j \in \mathcal{F} \\ T_i^{\mathrm{YAR}} - (\Delta^{\mathrm{Y^{RC}}} - \Delta^{\mathrm{EY^{RC}}} + \Delta^{\mathrm{Y^{WT}}}) & \text{otherwise} \end{cases} \tag{3.7}$$

T_i^{YAR} is the amount of electric energy that can be recharged at the last recharging station visited. It ensures that the maximum battery capacity is respected. If j is a recharging station, then the rechargeable amount is the difference between the maximum capacity Y and the current capacity of the battery (3.5). Otherwise, if j is a customer or the depot, the extended resource incorporates the amount of energy recharged in order to reach j (i.e., $\Delta^{\mathrm{Y^{RC}}} - \Delta^{\mathrm{EY^{RC}}}$) or used because of waiting time $\Delta^{\mathrm{Y^{WT}}}$. Second,

$$T_j^{\mathrm{TAR}} = \begin{cases} l_j - (e_0 + \Delta) & \text{if } j \in \mathcal{F} \\ \min\{T_i^{\mathrm{TAR}} - \Delta^{\mathrm{T^{RC}}} - \Delta^{\mathrm{Y^{WT}}} \cdot g, \max\{0, l_j - (e_0 + \Delta + \Delta^{\mathrm{WT}})\}\} & \text{otherwise} \end{cases} \tag{3.8}$$

T_i^{TAR} ensures that the required time warp due to lazy recharging operations is identified correctly. If $j \in \mathcal{F}$, the available recharging time is reset to the time remaining until the end of the time window. Otherwise, the minimum of two cases defines the extension: 1) the previous available time minus the time required to recharge in order to reach vertex v (i.e., $\Delta^{\mathrm{T^{RC}}}$) and due to waiting time ($\Delta^{\mathrm{Y^{WT}}} \cdot g$, where g is the inverse recharging rate), and 2) the remaining time window of the current customer. Finally, the intermediate

calculations are displayed below:

$$\Delta^{\mathrm{Y^{RC}}} = \max\{d_{ij} \cdot r_{\mathrm{E}} - T_i^{\mathrm{Y}}, 0\} \tag{3.9}$$

$$\Delta^{\mathrm{EY^{RC}}} = \max\{\Delta^{\mathrm{Y^{RC}}} - T_i^{\mathrm{Y}}, 0\} \tag{3.10}$$

$$\Delta^{\mathrm{T^{RC}}} = \Delta^{\mathrm{Y^{RC}}} \cdot g \tag{3.11}$$

$$\Delta^{\mathrm{TW^{RC}}} = \max\{\Delta^{\mathrm{T^{RC}}} - T_i^{\mathrm{TAR}}, 0)\} \tag{3.12}$$

$$\Delta = T_i^{\mathrm{DUR}} - T_i^{\mathrm{TW}} + \Delta^{\mathrm{T^{RC}}} - \Delta^{\mathrm{TW^{RC}}} + t_{ij} \tag{3.13}$$

$$\Delta^{\mathrm{WT}} = \max\{e_j - \Delta - e_0, 0\} \tag{3.14}$$

$$\Delta^{\mathrm{TW}} = \max\{e_0 + \Delta - l_j, 0\} \tag{3.15}$$

$$\Delta^{\mathrm{Y^{WT}}} = \min\{T_i^{\mathrm{YAR}} - \Delta^{\mathrm{Y^{RC}}}, \min\{T_i^{\mathrm{TAR}} - \Delta^{\mathrm{T^{RC}}}, \Delta^{\mathrm{WT}}\}/g\} \tag{3.16}$$

Equation (3.9) calculates the energy required to reach vertex v that is not covered by the energy stored in the battery (T_i^{Y}). The amount that is not rechargeable is calculated in (3.10) and depends on the charge available at the last recharging station visited (T_i^{YAR}). Equation (3.11) determines the time required for recharging the missing amount, and (3.12) stores the time warp required to satisfy the time window constraint. After this step, the actual duration is calculated using (3.13), which determines the waiting time and time warp occurring in vertex j. Equations (3.14) and (3.15) calculate the waiting time at vertex j and the time warp required, respectively. The second rule of our policy is enforced by (3.16), which determines the amount of recharging that can replace waiting at vertex j.

Greedy charging and mode selection policy (PHEV)

PHEVs pose an additional challenge because the availability of two engines introduces the need to select the propulsion mode. We assume that the mode can be changed at any time during the tour at no additional cost. Furthermore, the battery can be recharged in the same way as that of BEVs.

As for the BEV case, we assume that a completely sequenced route with possible recharging stations is provided. Our evaluation uses the following policy to decide the propulsion mode and to guarantee feasibility in time and energy, if possible:

- Use electric energy mode first;
- When a sequence ending in vertex i is extended by vertex j, and the energy required, $d_{ij} \cdot r_{\mathrm{E}}$, exceeds the current state, try to recharge the required amount at the last recharging station visited;
- Avoid waiting time by recharging;
- When a time window is violated, exchange the time spent recharging for the corresponding amount of fuel.

The first item comes directly from the assumption that electricity is cheaper than fossil fuel. Otherwise, no electricity would be required, reducing the problem to the variant with no energy constraints. The second and third points are identical to the BEV policy described above, ensuring that energy is recharged only when necessary or to avoid waiting time. In the BEV case, a time window can be violated because the vehicle arrives too late or charging is required. In contrast, a PHEV can use the ICE to avoid additional recharging time. This is handled by the last item of the policy. Of course, only recharging time can be reverted to avoid a time warp. A detailed description analogous to the BEV case can be found in the Appendix.

3.1.2. Second layer – Sequencing of recharging station visits

The planning of recharging-station visits is performed in a separate layer to decouple these decisions from the itinerary of customer visits. Given a fixed itinerary and the evaluation procedure described in the previous section, the remaining open question is which recharging station, if any, should be used between a sequence of fixed visits. This problem can be formulated as an RCSPP for a fixed sequence of customer visits. More details about the RCSPP, especially for the VRP, can be found in Irnich & Desaulniers (2005).

Let $\pi = \{v_0, v_1, v_2, \ldots, v_0\}$ be an itinerary without any recharging stations. The goal is to find the optimal recharging stations in $\mathcal{F}$ and their placement in π to obtain an energy and time feasible, cost minimal route

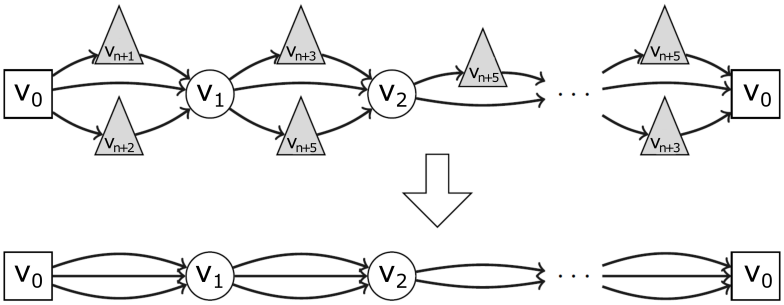

Figure 3.2: Transformation of the problem of finding the best path with recharging station visits to a fixed-sequence arc selection problem.

with possible recharging stations. The problem is transformable to the fixed-sequence arc selection problem described in Garaix et al. (2010) by representing each possible detour to a recharging station as a parallel arc in a directed acyclic multigraph; see Figure 3.2.

To solve this problem, we use a labeling algorithm following the general steps of Irnich & Desaulniers (2005) but differing in the label definition, the extension, and the dominance criterion. The description of the labeling algorithm uses a function-style notation to specify the value of a field of a label. The resources are defined specifically for each problem to ensure efficient handling of the dominance checks.

The resources for the BEV labeling are as follows:

$$R^{\text{BEV}} = \{v, T^{\text{COST}}, T^{\text{DUR}}, T^{\text{Y}}, T^{\text{YAR}}, T^{\text{TAR}}\}$$

where $T^{\text{COST}}(L)$ is the cost of the label, $T^{\text{DUR}}(L)$ the time duration at $v(L)$, and $T^{\text{Y}}(L)$ the current energy level. $T^{\text{YAR}}(L)$ is the rechargeable energy and $T^{\text{TAR}}(L)$ the maximum recharging time, both at the last recharging station visited. These values are taken directly from the results of the evaluation methods described in Section 3.1.1.

The dominance criterion is defined as follows: A label L_1 dominates L_2 if it has a lower cost (3.17), a shorter duration (3.18), and a higher maximal available energy (3.19), i.e., the current level plus the rechargeable amount. To further strengthen the criterion, we use Equation (3.20) in our dominance check. It states that the available electric energy must either be higher, or the total duration must be shorter after recharging the missing amount.

$$T^{\text{COST}}(L_1) \leq T^{\text{COST}}(L_2) \tag{3.17}$$

$$T^{\text{DUR}}(L_1) \leq T^{\text{DUR}}(L_2) \tag{3.18}$$

$$T^{\text{Y}}(L_1) + \min\{T^{\text{YAR}}(L_1), T^{\text{TAR}}(L_1) \cdot g\} \geq T^{\text{Y}}(L_2) + \min\{T^{\text{YAR}}(L_2), T^{\text{TAR}}(L_2) \cdot g\} \tag{3.19}$$

$$T^{\text{Y}}(L_1) \geq T^{\text{Y}}(L_2) \vee T^{\text{DUR}}(L_1) + (T^{\text{Y}}(L_2) - T^{\text{Y}}(L_1))/g \leq T^{\text{DUR}}(L_2) \tag{3.20}$$

For the PHEV, the labeling incorporates additional variables and several additional checks to strengthen the dominance check; see Appendix.

3.2. First Layer – Hybrid Genetic Search

To solve the assignment and sequencing problem at the first layer, we use a metaheuristic approach based on the HGA introduced in Vidal et al. (2012, 2013). The HGA variant in this paper has two additional components: 1) a set partitioning component to recombine routes encountered during the search process; 2) a destroy-and-recreate component, which acts as a fast mutation operator.

The general scheme is shown in Figure 3.3. Two populations are maintained during the search, containing either only feasible or only infeasible individuals. New individuals, called offspring, are generated at each iteration by one of three methods: 1) recombination (crossover), 2) mutation (destroy-and-recreate), or 3)

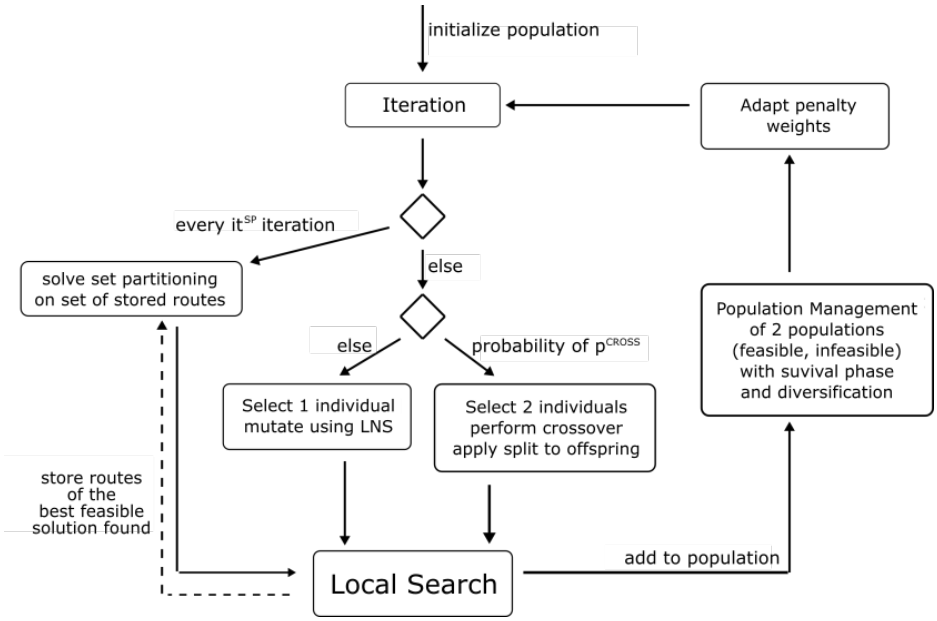

Figure 3.3: General overview of the HGA developed in this paper.

set partitioning. The set partitioning component is called every it^{SP} iterations, combining the routes found during the search. At every other iteration we perform either the recombination, with probability p^{CROSS}, or the mutation on individual(s) selected from both populations. After the offspring is generated, it is improved using an LS procedure and included in the appropriate population. Based on the size of the population and the performance of the search, survivor and diversification mechanisms are triggered.

The remainder of this section presents the components of the HGA in more details. Section 3.2.1 discusses the representation of a solution and the evaluation of individuals. Section 3.2.2 gives insight into the parent selection, recombination, and mutation. Section 3.2.3 presents the LS procedure, and Section 3.2.4 discusses the population management.

3.2.1. Solution representation and evaluation

A solution s is represented as a set of itineraries with an assigned vehicle type and class. These itineraries begin at the depot, visit customer vertices, and end at the depot. Recharging stations are present only in the evaluation data of the corresponding route, as described in Section 3.1.1.

Let $R(s)$ represent the routes in s, and let T_r be the computed evaluation data of each route $r \in R(s)$. A feasible solution does not allow any time window, energy, or capacity violations, i.e.,

$$(T_r^{\text{Q}} \leq Q^r) \wedge (T_r^{\text{EY}} \leq 0) \wedge (T_r^{\text{TW}} \leq 0) \tag{3.21}$$

where Q^r is the maximal load capacity of the vehicle assigned to route r. Infeasible solutions are obtained by relaxing the limits on the vehicle capacities, energy, and time-window violations. The objective value of a route r is defined as the combination of the general routing cost T_r^{COST} and the weighted sum of all violations, i.e.,

$$\text{OBJ}(r) = T_r^{\text{COST}} + \rho^{\text{Q}} \cdot (T_r^{\text{Q}} - Q^r) + \rho^{\text{EY}} \cdot T_r^{\text{EY}} + \rho^{\text{TW}} \cdot T_r^{\text{TW}} \tag{3.22}$$

where ρ^{Q} is the weight of the load capacity violations, ρ^{EY} the energy capacity violations, and ρ^{TW} the time window violations. The objective value $\text{OBJ}(s)$ of a solution s is calculated by summing the individual objectives $\text{OBJ}(s) = \Sigma_{r \in R(s)} \text{OBJ}(r)$.

To compute the fitness of a solution for an individual in the population, we use another metric to

determine the relative value of each individual with respect to the entire population. The fitness function used in this work is based on the original HGA proposed in Vidal et al. (2013), which combines the cost of an individual with its contribution to the population diversity.

The diversity contribution of an individual p is defined as the average distance to its μ^{CLOSE} most similar neighbors in the corresponding population $\mathcal{P}$. This distance is calculated using the broken-pair distance (Prins, 2009), which measures the proportion of common edges in the giant tour representation of an individual. The biased fitness function $f_{\mathcal{P}}(p)$ is shown in Equation (3.23). It is the weighted sum of the objective cost rank $f_{\mathcal{P}}^{\text{OBJ}}(p)$ and its rank $f_{\mathcal{P}}^{\text{DIV}}(p)$ relative to its diversity contribution. The balance of this trade-off between the objective and the diversity contribution is controlled by the parameter μ^{ELITE}.

$$f_{\mathcal{P}}(p) = f_{\mathcal{P}}^{\text{OBJ}}(p) + \left(1 - \frac{\mu^{\text{ELITE}}}{|\mathcal{P}|}\right) \cdot f_{\mathcal{P}}^{\text{DIV}}(p) \tag{3.23}$$

3.2.2. Generation of new individuals

An offspring of the current generation can be created by recombination, which applies a crossover operator to two parent individuals, or by mutation, which performs a single destroy-and-recreate step on a single individual. Each parent solution is selected using a binary tournament scheme, where two random individuals from the pool of feasible and infeasible solutions are compared, and the better one in terms of biased fitness is chosen. For recombination, this selection procedure is called twice to select two individuals.

Recombination.. Individuals of the HGA's population are recombined into their so-called giant tour representation. This is formed by concatenating all the routes and omitting the route-delimiters, i.e., visits to the depot. A giant tour is therefore simply an ordered permutation of all the customers. It can be used in simple recombination operators defined for permutations without any problem-specific adaptations. We use the OX crossover because of its good performance in other work (Prins, 2004; Vidal et al., 2012). To derive a complete solution from a giant tour, we apply a so-called split algorithm. It solves a shortest path problem to decide how to split the giant tour into subsequences and how to assign vehicle types. For the H^2E-FTW the split algorithm had to be slightly modified to test not only different vehicle types but also different classes. Other than that, it follows the same general steps of Prins (2004).

Mutation.. Our mutation operator is based on a large neighborhood search. A subset of vertices are removed from the current solution, and then reinserted using a greedy heuristic. Such "ruin-and-recreate" techniques have been shown to be remarkably efficient for a variety of vehicle routing problem variants (Ropke & Pisinger, 2006; Christiaens & Vanden Berghe, 2016).

The LNS embedded in our solver uses classical operators from the literature. Instead of an adaptive selection mechanism (Ropke & Pisinger, 2006), we use an uniform random selection of operators, which performed equally in our preliminary experiments. The set of destroy operators is as follows: a) random removal: the vertices removed are selected at random; b) random routes: complete routes are cleared at random; c) similar removal: pairs of similar vertices are removed, based on their distance values; and d) target removal: a single vertex is selected, and it is removed along with neighboring routes.

Two operators are used for solution reconstruction: a) a basic greedy insertion and b) a 2-regret insertion. The basic greedy insertion finds the best route and position for each vertex, and performs the best insertion based on the objective function. The regret insertion uses a regret value to decide which vertex to insert, based on the difference between the best and the second best insertion positions.

The evaluation of removals and insertions in the LNS component differs from the systematic evaluation described in Section 3. It uses an explicit representation of the routes, i.e., recharging station visits are heuristically included as part of the reconstruction instead of the evaluation method. This change was applied after preliminary tests indicated that an explicit representation resulted in a significant decrease in computational effort with no significant decrease in the solution quality.

3.2.3. Improvement by local search

The solution generated at each iteration using recombination, mutation, or set partitioning is improved using an LS procedure extended with a repair mechanism proposed in Vidal et al. (2012). The LS scans

the set of moves in random order. Any improving move is immediately applied, and the process is repeated until no such move can be found. If the improved solution is feasible (see Section 3.2.1), no additional action is performed. Otherwise, it is considered for a heuristic repair step with a probability of p^{REPAIR}, where the penalty weights are multiplied by 10 temporarily, and the LS is restarted. If it is still infeasible, another run with the weights multiplied by 100 is performed. No further attempts are made, and the local procedure terminates.

Neighborhood search.. We use three neighborhood search operators: 2-opt, 2-opt*, and cross-exchange. The 2-opt operator is an intra-route operator; it works with a single route and inverts a subsequence. The 2-opt* operator works with two routes, splitting each into two parts and then reconnecting them differently. The cross-exchange operator swaps consecutive portions of two routes; to reduce the computational effort, at most two consecutive vertices are swapped.

Neighborhood restrictions.. The number of neighbors is large, so we use a pruning approach to restrict the search space. We calculate a set of so-called *promising* edges for each customer vertex (Vidal et al., 2013). Only the moves generating at least one promising edge are tested. Equation (3.24) defines a *customer correlation* measure, used to determine this set.

$$\begin{aligned}\gamma(i,j) = d_{ij} &+ \gamma^{\text{WT}} \cdot \max(e_j - s_i - t_{ij} - l_i, 0) \\ &+ \gamma^{\text{TW}} \cdot \max(e_i + s_i + t_{ij} - l_j, 0)\end{aligned} \tag{3.24}$$

As seen in Equation (3.24), the set of promising edges from a customer v_i is based on direct distance, unavoidable waiting time (γ^{WT})and time-window violation (γ^{TW}). The final set of *promising* arcs $\Gamma(i)$ consists of the $|\Gamma|$ closest customers v with respect to the correlation measure $\gamma(i,j)$. The same settings as Vidal et al. (2013) are used: $|\Gamma| = 40$, $\gamma^{\text{WT}} = 0.2$, and $\gamma^{\text{TW}} = 1.0$.

Lower bounds on move evaluations.. To avoid systematic calls to the computationally expensive DP procedure for BEV or PHEV route evaluations, we use lower bounds on move evaluations, as proposed in Vidal (2017), to filter a large proportion of candidate moves. To compute a fast lower bound, we treat a BEV (PHEV) as a simple ICEV but apply the electricity cost of the electric engine. Therefore, any move is first evaluated as an ICEV in $\mathcal{O}(1)$ operations, (effectively ignoring recharging stations) and compared to the current BEV (PHEV) route cost. If the move leads to a better objective, then the original BEV (PHEV) calculations are performed to determine the true value of the move. Otherwise, the move cannot lead to a better solution and is discarded.

Memory.. During the move evaluation, a cache memory is maintained where move changes can be stored and retrieved in subsequent evaluations if they are still valid. Validity is ensured by purging the move-evaluation values of affected routes after a move. This technique also leads to a considerable reduction in the computational time.

3.2.4. Population management

We maintain two populations during the search, one with only feasible solutions and the other with only infeasible ones. Each population contains up to $\mu^{\text{MIN}} + \mu^{\text{GEN}}$ individuals. Whenever the population exceeds this number, a survivor-selection process is initialized to reduce the population to μ^{MIN}. This procedure sorts the solution based on the biased fitness described in Section 3.2.1 and removes the last μ^{GEN} individuals.

The two populations are initialized by generating μ^{INIT} at the beginning of the search, applying local search and repair with a probability of p, and inserting them into the appropriate population. To diversify the search, a diversification phase is triggered after each it^{DIV} iterations without improvement of the best solutions. It removes all but the best μ^{ELITE} solutions and creates μ^{div} new random solutions, adding them to the corresponding population.

A solution is called naturally feasible if it is feasible after the LS procedure of Section 3.2.3. During the search, the penalties introduced in Section 3.2.1 are adapted to give a targeted proportion of naturally feasible solutions ξ^{REF}. Let ξ^{Q} and ξ^{TW} be the proportion of naturally feasible solutions with regards to the

load and time-window constraints respectively. The following adjustment is performed every 20 iterations, where $c \in \{\text{Q}, \text{TW}\}$:

$$\rho^{\text{C}} = \begin{cases} \rho^{\text{C}} \cdot 1.20 & \text{if } \xi^c \leq \xi^{\text{REF}} - 0.05 \\ \rho^{\text{C}} \cdot 0.85 & \text{if } \xi^c \geq \xi^{\text{REF}} + 0.05 \end{cases} \tag{3.25}$$

3.2.5. Set partitioning

The algorithm encounters many different routes during its search. To exploit this history, we embed a procedure to store and combine a subset of these routes. Such methods have been successfully applied in the past, leading to promising results for related problems (Subramanian et al., 2013).

At the end of every iteration of the HGA, the routes of the current local minimum are stored in an archive, together with the objective value and the overall solution quality. To avoid duplicates, a hash value is calculated based on the itinerary of the route, and the entry is replaced if a better route is encountered, i.e., using another vehicle class or type. To restrict the memory usage and performance penalty, the size of this archive is bounded by λ. After a solution is added, if the bound is exceeded, around half of the stored routes are removed from the archive. This purge is biased based on the quality of the corresponding route. More details on the hashing calculation and the purging can be found in Goel & Vidal (2014).

Every it^{SP} iterations a set partitioning problem is formulated with the routes available in the archive. The solution of this problem is a subset of routes with no overlapping customer assignments. We use partitioning instead of covering to avoid the need to repair overlapping assignments. The problem is solved using a commercial MIP solver. To improve the quality of the procedure, additional routes are generated during a preprocessing step with a single customer vertex; these are added to the formulation.

4. Experiments

Extensive experiments have been conducted in order to evaluate the performance of the HGA approach, and to gain managerial insights for the management of an hybrid fleet with different propulsion modes. All our experiments were run on a single thread of an Intel Xeon 2643 3.3 GHz core, using a maximum RAM of 4 GB. We use CPLEX 12.6 for the solution of the set partitioning problems. The HGA was implemented in Java 8 and run using the Java Runtime Environment 1.8, Update 20 (JRE 8u20). We performed ten test runs for each instance, and report average and best results.

4.1. H^{2}E-FTW benchmark set

We first created a H^{2}E-FTW benchmark set as a basis for the analysis of the metaheuristic and its components, as well as to allow for future comparisons. These instances are based on the 56 homogeneous electric fleet instances of Schneider et al. (2014), each with a single depot, 100 customers and 21 recharging stations. They are divided into six categories, based on their spatial (c, r, rc) and temporal (type-1, type-2) configurations. Instances of category (c) contain several clusters of customers. In (r) instances, customers are uniformly distributed, and (rc) instances consist of some clusters and some uniformly distributed customers. Type-1 instances have smaller time windows, whereas type-2 instances have larger ones as well as bigger vehicle capacities.

Each instance has been extended by adding a set of vehicle types and classes. The parameters of the vehicles are derived from a German study of the electric vehicle market (Plötz et al., 2013), in which the authors aggregated the different vehicle types into four categories: small, medium, large, and others. For these categories, average values are given for the parameters required in our work, e.g., consumption rate, battery size, and acquisition cost. We used the values of the first three categories (small, medium and large) for each of the three vehicle classes (ICEV, PHEV, BEV) to generate our instances.

Since the original E-VRPTW instances are based on artificial VRPTW instances, some adjustments had to be made. First, we used the properties provided in the E-VRPTW instance files and assumed that the original vehicle is in the "large" category. The remaining vehicles types were derived by fixing this baseline and using the relative differences from Plötz et al. (2013). Finally all distances were scaled in such a way that one unit of distance represents one kilometer.

4.2. Parameter calibration

Subsequently, we performed a calibration of the method's parameters. To avoid over-tuning, we used a randomly selected subset of instances: c101, r104, rc102, rc108, c203, r202, r205, and rc202. We identified a subset of parameters with a larger effect on the performance of the algorithm. These are: the population size μ, the number of iterations it^{MAX}, the crossover probability p^{CROSS} (which is the same as the crossover-to-mutation ratio), the number of nonimproving iterations before diversifying it^{DIV}, the diversification ratio μ^{DIV}/μ, and the maximum time warp allowed for a label to stay in the undominated label set $L^{\text{TW}^{\text{MAX}}}$.

We first conducted preliminary experiments to converge towards suitable values for these parameters, leading us to the configuration marked with an asterisk (*) in Table 4.1. Then, we varied each parameter, one factor at time (OFAT approach), while fixing the others. This led us to several alternative configurations which are also reported in the table. These results allow to visualize the individual impact of each parameter, and highlights some clear trade-offs between solution quality and CPU time. The final parameters were selected to balance these two performance indicators, as shown in Table 4.2.

μ	4	8	15*	25
obj	1945.99	1944.75	**1943.59**	1945.14
t[s]	**691.75**	751.04	854.58	1013.92
it^{MAX}	500	1000	1500*	2000
obj	1966.65	1953.18	1943.59	**1942.48**
t[s]	**261.45**	557.27	854.58	1170.02
p^{CROSS}	0.2	0.4*	0.6	0.8
obj	1951.56	1943.59	1939.44	**1934.35**
t[s]	**785.28**	854.58	931.15	972.97
it^{DIV}	50	100*	200	500
obj	1944.38	1943.59	**1941.36**	1948.55
t[s]	1075.62	854.58	733.69	**705.29**
μ^{DIV}/μ	0.5	1*	1.5	2
obj	1944.73	**1943.59**	1946.31	1944.23
t[s]	**772.74**	854.58	950.34	1034.05
$L^{\text{TW}^{\text{MAX}}}$	0	200*	2000	
obj	2039.65	1943.59	**1942.61**	
t[s]	**611.36**	854.58	1073.78	

Table 4.1: Parameter calibration results from settings derived from preliminary experiments. Values marked with * were used as the base setting for this setup.

it^{MAX}	1500	μ	8
it^{SP}	25	μ^{INIT}	5
t^{SP}	10s	μ^{ELITE}	3
p^{CROSS}	0.4	it^{DIV}	200
p^{REPAIR}	0.5	μ^{DIV}/μ	0.5
LNS^{MAX}	10	$L^{\text{TW}^{\text{MAX}}}$	200
LNS^{MIN}	30		

Table 4.2: Parameter settings after calibration.

Finally, for the experiments with different cost values for fuel and electricity usage, we will consider the following scenarios: the electric energy cost can be [0.1, 0.3, 0.5, 0.7] monetary units per unit (kW) consumed, and fuel cost can be [1.0, 1.5, 2.0, 2.5, 3.0, 4.0] monetary units per unit (liter).

4.3. Sensitivity Analysis – Components of the Method

Table 4.3 compares different compositions of the method components described in Section 3.2. The first three rows show which components are active in the corresponding run. The fourth row reports the average results over all ten runs, and the fifth row gives the average CPU time in seconds. The adjacent percentage gives the deviation from the base setting (first column). Deactivating any component leads to a deterioration of between 1% and 3% of the average objective value found by the solver. The time differences are larger:

deactivating the crossover results in a decrease of one third. On the other hand, deactivating the LNS gives a slight decrease in the objective value and increases the CPU time by 15%. This is due to the fact that the LNS as described in Section 3.2 relies on an explicit representation of the recharging stations in the routes, thus avoiding the time-consuming labeling procedure. We kept the faster approach, therefore with LNS, for the remainder of the experiments.

Cross	X	X				X		X		
LNS	X			X		X			X	
SP	X					X		X		
obj_{avg}	1947.57	1976.20	1.47%	2003.79	2.89%	1994.57	2.41%	1937.39	-0.52%	1970.32	1.17%
$t[s]$	897.02	975.38	8.74%	675.99	-24.64%	705.53	-28.52%	1035.20	15.40%	862.94	-3.80%

Table 4.3: Analysis of the components involved, showing the average objective value and CPU time. The percentages next to the values show the deviation from the base setting (left column).

4.4. Sensitivity Analysis – Fleet composition

We have formulated a fleet mix problem with different vehicle classes, ICEV, PHEV, and BEV. To assess the benefits of fleet-mix optimization and the impact of different vehicle classes, we performed experiments restricting the fleet to a single class. Table 4.4 and Figure 4.1 show this comparison. For each cost value of the respective metric (c_{E} – electricity cost, c_{F} – fuel cost) 10 runs of each single class case are compared to runs from the mixed case.

		All			ICEV			BEV			PHEV		
		Obj	Gap	#Veh	Obj	Gap	#Veh	Obj	Gap	#Veh	Obj	Gap	#Veh
c_{E}	0.10	1543.69	0.00%	8.17	1932.88	25.21%	7.95	1637.46	6.07%	8.06	1660.90	7.59%	9.27
	0.30	1683.28	0.00%	7.81	1933.67	14.88%	7.96	1806.49	7.32%	7.99	1808.51	7.44%	8.90
	0.50	1770.44	0.00%	7.56	1937.95	9.46%	7.97	1986.22	12.19%	7.91	1930.59	9.05%	8.69
	0.70	1816.56	0.00%	7.43	1931.98	6.35%	7.94	2199.41	21.08%	7.89	2032.41	11.88%	8.65
c_{F}	1.00	1445.51	0.00%	7.29	1527.95	5.70%	7.71	1909.96	32.13%	7.79	1641.40	13.55%	8.91
	1.50	1569.98	0.00%	7.41	1686.38	7.41%	7.83	1897.81	20.88%	7.82	1734.58	10.48%	8.82
	2.00	1679.62	0.00%	7.56	1837.54	9.40%	7.91	1884.77	12.21%	7.88	1822.17	8.49%	8.76
	2.50	1768.62	0.00%	7.77	1991.89	12.62%	7.97	1912.76	8.15%	7.97	1899.43	7.40%	8.88
	3.00	1838.10	0.00%	8.00	2135.65	16.19%	8.05	1910.79	3.95%	8.08	1967.41	7.03%	8.90
	4.00	1919.12	0.00%	8.42	2425.31	26.38%	8.24	1928.28	0.48%	8.25	2083.62	8.57%	9.00

Table 4.4: Comparison of results for individual vehicle classes and all classes.

The gap for the ICEV case is growing with increasing fuel cost with more than 60% on average for the extreme case ($c_{\text{E}} = 0.1$, $c_{\text{F}} = 1.0$). BEV gaps grow with increasing electricity costs, up around 40% on average. In case of PHEV, the gaps remain rather small for most settings. However, in case of either low electricity or low fuel cost, the gap increases up to 25%. This can be due to the higher utility cost of PHEVs compared to the other classes.

In addition, Table 4.5 shows detailed results for a single cost setting ($c_{\text{E}} = 0.3$, $c_{\text{F}} = 2.0$). We chose the one with the most evenly spread fleet mix on average. The results show that more BEVs are used in c type instances, whereas more ICEVs are used in (r) and (rc) type instances. For the type-1 instances we see that a mix of vehicles produced the best results. However, with larger time windows, as in the type-2 instances, a clearer preference is visible, especially in the r instances, where PHEVs are used almost exclusively.

4.5. Sensitivity Analysis – Cost factors

We now investigate the impact of fuel and electricity cost on optimized fleet compositions and operational costs. Table 4.6 shows the average gap in the objective value compared to high electricity cost, low fuel cost scenario ($c_{\text{E}} = 0.7$, $c_{\text{F}} = 1.0$). Figure 4.2 presents the corresponding average vehicle class usage over all runs of all instances.

The gap is nearly zero in all other electricity cost settings but the smallest with 0.1, where the gap is negative with -3%. By using a higher fuel cost value of 4.0, the gap increases to 47.65%. The increase is

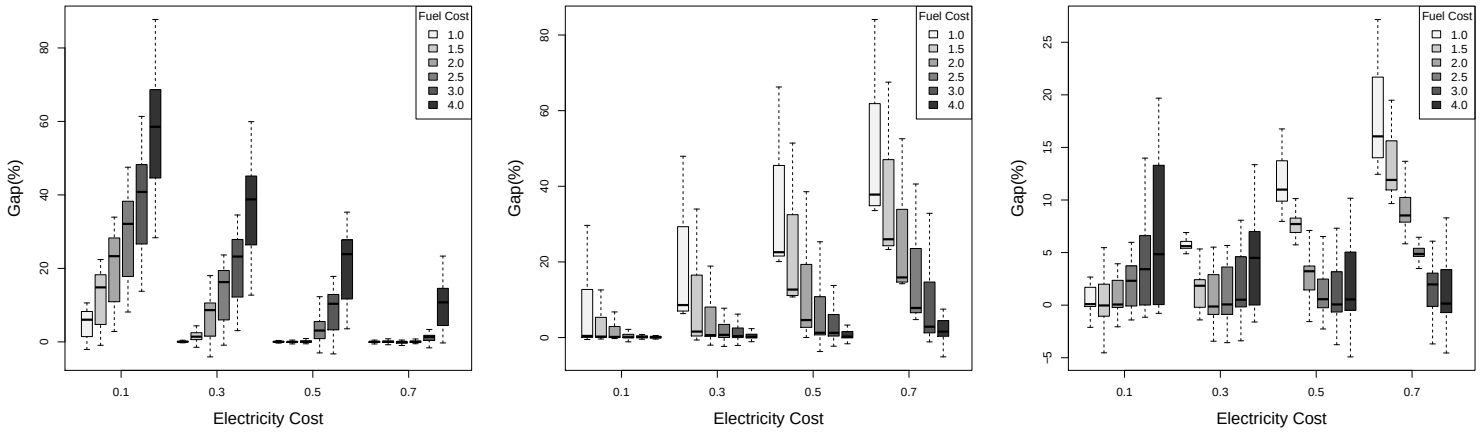

Figure 4.1: Gap(%) of the solutions obtained with an homogeneous fleet of ICEV (left), BEV (middle), and PHEV (right), relative to the optimized solution with a mixed fleet.

Name	Best 10	Avg 10	T(min)	I	P	B	Name	Best 10	Avg 10	T(min)	I	P	B
c101	2484.52	2486.10	6.47	0.4	0.8	10.8	c201	832.80	833.81	11.89	0.0	0.0	4.0
c102	2324.03	2380.20	7.40	1.6	1.2	8.1	c202	830.82	833.19	13.76	0.0	0.0	4.0
c103	2290.92	2317.66	8.35	1.1	2.5	6.8	c203	827.49	828.60	16.22	0.0	0.0	4.0
c104	2209.32	2215.73	9.47	1.3	2.0	6.7	c204	823.84	823.98	16.88	0.0	0.0	4.0
c105	2373.39	2410.22	6.78	1.4	3.1	6.3	c205	824.43	824.43	12.97	0.0	0.0	4.0
c106	2372.68	2404.75	7.27	1.3	2.6	7.0	c206	824.57	824.57	14.29	0.0	0.0	4.0
c107	2351.41	2396.50	6.93	1.4	2.2	7.3	c207	824.18	824.18	14.30	0.0	0.0	4.0
c108	2321.09	2346.54	7.70	1.6	3.5	5.2	c208	824.64	824.64	13.72	0.0	0.0	4.0
c109	2248.84	2277.38	7.72	0.7	2.8	6.7							
r101	3561.46	3602.19	7.57	12.4	1.2	2.7	r201	640.68	642.29	18.00	0.0	3.0	0.0
r102	3240.81	3258.85	8.05	10.7	1.4	2.9	r202	582.49	583.14	19.72	0.0	3.0	0.0
r103	2781.05	2818.80	8.63	9.6	1.0	1.7	r203	592.12	593.93	23.98	0.0	3.0	0.0
r104	2437.22	2468.18	10.23	7.3	1.5	1.6	r204	425.81	427.67	39.59	0.0	2.0	0.0
r105	2979.09	2991.25	7.77	10.6	1.0	1.4	r205	597.00	598.67	25.57	0.0	3.0	0.0
r106	2806.32	2817.29	9.04	9.9	1.5	0.6	r206	600.59	601.79	31.11	0.0	3.0	0.0
r107	2456.63	2528.41	9.14	7.8	0.9	1.9	r207	425.55	427.86	38.82	0.0	2.0	0.0
r108	2329.04	2385.74	9.43	7.8	0.8	1.2	r208	432.17	433.94	40.03	0.0	2.0	0.0
r109	2616.63	2651.03	7.78	8.6	1.0	1.6	r209	592.21	593.73	29.99	0.0	3.0	0.0
r110	2389.62	2449.35	9.35	8.3	0.3	1.7	r210	585.77	586.92	32.27	0.0	3.0	0.0
r111	2436.30	2479.86	9.37	8.2	1.1	0.9	r211	425.90	443.39	44.17	0.0	2.0	0.1
r112	2366.37	2382.81	9.28	8.1	1.1	0.8							
rc101	3159.62	3212.67	7.53	6.1	2.1	6.5	rc201	800.61	801.43	18.18	0.0	4.0	0.0
rc102	2974.32	3029.84	8.02	4.9	3.7	5.0	rc202	618.81	620.69	23.07	0.0	2.9	0.1
rc103	2644.37	2712.23	8.48	4.7	3.0	4.2	rc203	617.31	620.22	24.79	0.0	3.0	0.0
rc104	2423.23	2459.12	9.47	4.3	3.7	2.2	rc204	634.61	638.10	26.13	0.0	2.9	0.1
rc105	2889.19	2907.22	7.65	5.2	3.2	4.6	rc205	659.20	695.54	20.95	0.2	2.3	0.5
rc106	2761.25	2791.56	8.12	5.4	3.6	3.2	rc206	622.83	625.01	24.25	0.0	3.0	0.0
rc107	2543.54	2571.74	8.71	4.5	3.6	3.0	rc207	609.47	613.20	30.83	0.0	2.9	0.1
rc108	2446.58	2485.15	8.70	3.3	3.6	3.8	rc208	623.79	626.71	34.28	0.0	2.5	0.5

Table 4.5: Detailed results for each instance with fixed costs (electricity: 0.30, fuel: 2.00): best and average objective value, average CPU time in minutes, and average number of vehicles per class (I: ICEV, P: PHEV, and B: BEV).

$c_E \setminus c_F$	1.00	1.50	2.00	2.50	3.00	4.00
0.10	-3.00%	1.28%	3.59%	4.93%	5.83%	6.69%
0.30	0.01%	8.75%	14.58%	18.09%	19.82%	21.72%
0.50	-0.05%	9.52%	19.31%	26.63%	31.24%	36.17%
0.70	0.00%	9.55%	19.43%	28.81%	37.64%	47.65%

Table 4.6: Gap in the objective value for different cost values compared to the cost combination (electricity: 0.70, fuel: 1.00).

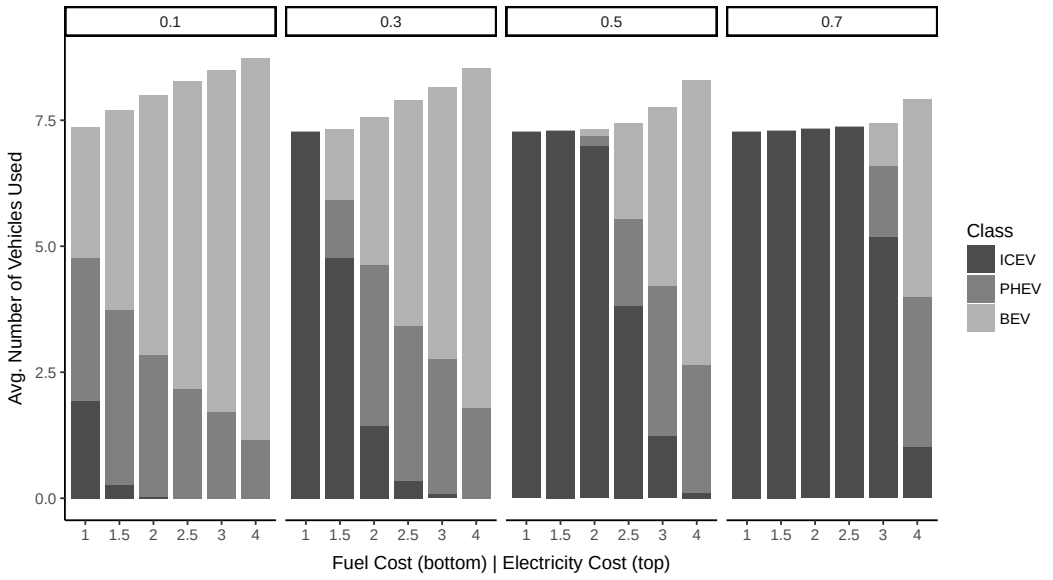

Figure 4.2: Change in the fleet composition for different cost values.

steeper in the the lower value settings, with almost 10% per step, e.g., in scenario ($c_{\mathrm{E}} = 0.7$, $c_{\mathrm{F}} = 1.5$) and ($c_{\mathrm{E}} = 0.7$, $c_{\mathrm{F}} = 2.0$). The reason for this can be observed in Figure 4.2. In the low fuel cost scenarios with higher electricity cost ($c_{\mathrm{E}} = 0.5$, $c_{\mathrm{E}} = 0.7$), the number of vehicles is not increasing and almost all vehicles in the mix are ICEVs. The gap increase is caused only by the increase in the fuel cost. When the increase is less steep, e.g., between scenario ($c_{\mathrm{E}} = 0.5$, $c_{\mathrm{F}} = 2.0$) and ($c_{\mathrm{E}} = 0.5$, $c_{\mathrm{F}} = 2.5$) with around 7%, we can observe a shift in the fleet mix towards electric vehicles.

We can also observe the inverse with the electricity cost where an increase leads to a full switch to an ICEV-only fleet. This happens instantly between scenario ($c_{\mathrm{E}} = 0.1$, $c_{\mathrm{F}} = 1.0$) and ($c_{\mathrm{E}} = 0.3$, $c_{\mathrm{F}} = 1.0$). In these scenarios the higher utility costs of BEVs become a key factor compared to the very cheap fuel.

Note that PHEVs are rarely the largest component of a fleet on average. This may be due to their generally higher utility cost and the higher consumption rates compared to similar ICEVs and BEVs. However, due to their increased flexibility, they still play a role in many optimized fleet configurations, representing 20% of the overall number of vehicles used in the solutions.

4.6. Performance Analysis – E-VRPTW(PR)

The E-VRPTW is the seminal problem in the field of electric vehicle routing with recharging stations. It defines a fixed recharging policy, where the BEV is always recharged to full capacity at a recharging station. This assumption was relaxed by Keskin & Çatay (2016), resulting in the E-VRPTW with partial recharging (E-VRPTWPR). Both formulations aim first to optimize the number of vehicles used and then to decrease the total distance of the routes. To achieve this, we assigned a high fixed cost ($f^k = 2000$) for the use of a vehicle. Moreover, minor modifications were applied to the second and third route evaluation layers to respect the fixed recharging scheme. To calculate the objective value, we use the extension function described in Hiermann et al. (2016). The dominance criterion is adapted accordingly.

Table 4.7 and 4.8 show the results for the E-VRPTW and E-VRPTWPR benchmark instances. Our results are similar to those in the literature, on average within around 0.2% of the best known solutions. We found 11 new best solutions, the majority in the type-1 category, which have tighter time windows.

The average CPU time of our solver is 11.59 min for the E-VRPTW. This performance is competitive; in the literature, time values of 15.34 min (Schneider et al., 2014), 15.92 min (Hiermann et al., 2014), and 12.26 min (Keskin & Çatay, 2016) are reported. Goeke & Schneider (2015) reported an average CPU time of 2.78 min, but as noted by Keskin & Çatay (2016), their algorithm uses *a priori* information on the number of vehicles, which makes a meaningful comparison difficult.

Name	**SSG** Best 10	**HPH** Best 10	**GS** Best 10	**KÇ** Best 10	**HGA** Avg 10	**HGA** Best 10	**HGA** T(min)	**BKS**
c101	**12/1053.83**	**12/1053.83**	**12/1053.83**	**12/1053.83**	**12.0/1053.83**	**12/1053.83**	3.81	12/1053.83
c102	11/1057.21	11/1057.21	11/1057.21	11/1056.12	11.0/1057.45	11/1055.12	5.37	11/1051.38
c103	10/1041.55	10/1044.15	10/1038.84	11/1001.81	10.6/1020.22	**10/1034.86**	9.93	10/1034.86
c104	10/980.78	10/984.60	10/972.07	**10/951.57**	10.0/958.91	10/953.63	10.07	10/951.57
c105	**11/1075.37**	**11/1075.37**	**11/1075.37**	**11/1075.37**	11.0/1076.71	**11/1075.37**	4.65	11/1075.37
c106	**11/1057.86**	**11/1057.65**	**11/1057.65**	**11/1057.65**	11.0/1058.17	**11/1057.65**	5.25	11/1057.65
c107	**11/1031.56**	**11/1031.56**	**11/1031.56**	**11/1031.56**	11.0/1033.44	**11/1031.56**	7.00	11/1031.56
c108	10/1100.32	10/1109.45	10/1098.89	11/1015.68	11.0/1015.68	11/1015.68	8.47	10/1095.66
c109	10/1051.88	10/1051.46	10/1033.63	10/1069.16	10.4/1044.71	10/1060.78	11.26	10/1033.67
c201	**4/645.16**	**4/645.16**	**4/645.16**	**4/645.16**	**4.0/645.16**	**4/645.16**	5.38	4/645.16
c202	**4/645.16**	4/646.51	**4/645.16**	**4/645.16**	**4.0/645.16**	**4/645.16**	7.59	4/645.16
c203	**4/644.98**	**4/644.98**	**4/644.98**	**4/644.98**	4.0/645.00	**4/644.98**	7.93	4/644.98
c204	**4/636.43**	4/638.34	**4/636.43**	**4/636.43**	4.0/636.92	**4/636.43**	8.57	4/636.43
c205	**4/641.13**	**4/641.13**	**4/641.13**	**4/641.13**	**4.0/641.13**	**4/641.13**	6.46	4/641.13
c206	**4/638.17**	**4/638.17**	**4/638.17**	**4/638.17**	**4.0/638.17**	**4/638.17**	7.32	4/638.17
c207	**4/638.17**	**4/638.17**	**4/638.17**	**4/638.17**	**4.0/638.17**	**4/638.17**	7.56	4/638.17
c208	**4/638.17**	**4/638.17**	**4/638.17**	**4/638.17**	**4.0/638.17**	**4/638.17**	7.54	4/638.17
r101	**18/1672.52**	**18/1663.04**	18/1670.69	18/1679.06	18.0/1664.50	**18/1663.04**	7.74	18/1663.04
r102	16/1535.87	16/1488.97	16/1492.84	16/1519.80	**16.0/1486.99**	**16/1484.57**	7.95	16/1487.41
r103	13/1299.59	13/1285.96	13/1281.97	13/1312.50	13.2/1284.47	**13/1268.88**	11.89	13/1271.35
r104	**11/1088.43**	11/1097.79	11/1090.72	12/1071.89	11.7/1090.68	11/1103.50	14.74	11/1088.43
r105	14/1473.52	15/1433.92	14/1453.80	15/1383.29	15.0/1394.63	15/1382.70	13.56	14/1442.35
r106	13/1344.66	13/1363.22	13/1359.85	14/1276.15	14.0/1275.88	14/1275.86	14.95	13/1324.10
r107	12/1154.52	12/1165.37	12/1151.52	12/1148.43	12.0/1163.54	**12/1148.38**	13.78	12/1148.43
r108	11/1065.90	11/1067.47	11/1062.85	11/1051.59	11.0/1064.58	**11/1049.12**	15.23	11/1050.04
r109	12/1294.05	13/1245.91	12/1261.31	13/1214.72	13.0/1228.37	13/1214.63	14.43	12/1261.31
r110	11/1143.53	11/1155.58	11/1141.39	12/1097.89	12.0/1103.46	12/1097.66	15.22	11/1119.50
r111	12/1124.11	12/1120.46	12/1124.00	12/1109.14	12.0/1111.12	**12/1099.53**	14.72	12/1106.19
r112	11/1026.52	11/1043.77	11/1026.73	11/1038.74	11.1/1023.78	**11/1016.63**	14.25	11/1016.63
r201	**3/1264.82**	3/1269.50	3/1267.48	3/1265.67	3.0/1273.88	3/1267.14	9.81	3/1264.82
r202	**3/1052.32**	3/1053.90	3/1052.85	**3/1052.32**	3.0/1053.45	**3/1052.32**	10.96	3/1052.32
r203	3/912.84	3/897.16	3/899.05	**3/895.54**	3.0/910.15	**3/895.54**	12.35	3/895.54
r204	2/790.56	2/788.67	2/782.91	2/780.98	2.0/795.91	2/784.77	19.19	2/779.49
r205	3/988.67	3/1002.02	3/990.05	**3/987.36**	3.0/995.02	**3/987.36**	11.51	3/987.36
r206	3/925.19	3/922.70	3/924.82	3/922.70	3.0/932.97	3/925.34	14.18	3/922.19
r207	2/852.69	2/859.82	2/848.95	2/847.14	2.0/851.73	2/847.59	18.08	2/845.26
r208	2/736.60	2/740.21	2/739.84	**2/736.12**	2.0/739.11	**2/736.12**	17.26	2/736.12
r209	3/872.36	3/890.68	3/873.76	3/871.22	3.0/873.64	3/870.68	16.82	3/867.05
r210	3/847.06	3/863.49	3/849.94	**3/843.65**	3.0/850.48	3/846.62	17.86	3/843.65
r211	2/866.18	2/873.64	2/835.50	3/761.56	2.3/834.94	2/836.27	19.45	2/827.89
rc101	16/1731.05	16/1726.91	16/1735.03	16/1731.07	**16.0/1723.79**	**16/1723.79**	13.02	16/1726.91
rc102	15/1554.65	**14/1659.53**	15/1557.47	15/1551.69	15.0/1553.15	15/1551.28	14.57	14/1659.53
rc103	13/1353.58	13/1369.39	13/1351.42	13/1351.73	13.0/1350.98	13/1350.55	14.86	13/1350.09
rc104	11/1249.25	11/1229.82	11/1229.21	11/1232.45	11.3/1235.85	11/1230.92	13.46	11/1227.25
rc105	14/1483.42	14/1478.70	14/1484.46	**14/1473.24**	14.0/1476.84	**14/1473.24**	12.13	14/1475.31
rc106	13/1440.20	13/1436.61	13/1439.05	14/1414.99	13.0/1433.67	**13/1423.27**	9.81	13/1427.21
rc107	12/1275.89	12/1283.55	12/1276.40	12/1283.05	12.0/1278.56	**12/1274.41**	13.72	12/1274.89
rc108	11/1238.85	11/1204.87	11/1200.65	11/1209.11	11.0/1203.61	**11/1197.41**	8.92	11/1197.83
rc201	**4/1447.25**	4/1464.30	4/1446.82	4/1446.84	4.0/1454.23	4/1446.03	10.10	4/1444.94
rc202	3/1412.91	3/1437.07	3/1419.27	3/1450.34	3.0/1430.52	3/1421.34	11.78	3/1410.74
rc203	3/1078.28	3/1084.72	3/1073.87	3/1069.27	3.0/1069.15	3/1057.16	11.52	3/1055.19
rc204	3/889.25	3/902.70	3/892.43	3/887.45	3.0/888.20	**3/884.72**	13.12	3/884.80
rc205	3/1321.70	3/1282.58	3/1289.76	3/1277.60	3.4/1236.75	3/1280.33	12.68	3/1273.55
rc206	3/1191.11	3/1218.73	3/1191.46	3/1207.64	3.0/1209.22	3/1190.50	11.11	3/1188.63
rc207	3/995.52	3/1016.13	3/1005.57	3/994.48	3.0/1002.13	3/991.96	12.78	3/985.03
rc208	3/838.07	3/847.87	3/836.31	3/841.34	3.0/839.99	**3/836.29**	15.23	3/836.29
Time	15.34 min	15.92 min	2.78 min*				11.59	
Gap	0.23/0.45	0.45/1.00	0.23/0.38	2.27/-0.34	2.05/-0.16	1.36/-0.46		

Table 4.7: Comparison with the results for the E-VRPTW of Schneider et al. (2014). SSG: Schneider et al. (2014); HPH: Hiermann et al. (2014); GS: Goeke & Schneider (2015); KÇ: Keskin & Çatay (2016)

For the E-VRPTWPR, the average CPU time is 11.29 minutes compared to 16.77 minutes as reported by Keskin & Çatay (2016). We found 28 new best solutions and six solutions that reduced the number of vehicles. Most improvements occurred in the r and rc variants, in both the type-1 and type-2 categories.

Name	KÇ Best 10	HGA Avg 10	HGA Best 10	HGA T(min)	BKS
c101	12.0/1051.23	**12.0/1044.511**	**12.0/1044.511**	3.44	12.0/1051.23
c102	11.0/1034.24	11.0/1033.795	**11.0/1033.795**	4.42	11.0/1034.24
c103	**10.0/973.39**	10.0/1001.127	10.0/1001.127	5.78	10.0/973.39
c104	**10.0/886.72**	10.0/893.0406	10.0/893.0406	6.96	10.0/886.72
c105	**11.0/1037.78**	11.0/1052.948	11.0/1052.948	3.78	11.0/1037.78
c106	**11.0/1024.18**	11.0/1043.503	11.0/1043.503	4.70	11.0/1024.18
c107	**10.0/1058.11**	11.0/1013.761	11.0/1013.761	4.69	10.0/1058.11
c108	**10.0/1033.5**	11.0/1000.555	11.0/1000.555	7.31	10.0/1033.5
c109	10.0/960.03	**10.0/946.8438**	**10.0/946.8438**	5.16	10.0/960.03
c201	**4.0/629.95**	4.0/658.1089	4.0/658.1089	4.93	4.0/629.95
c202	**4.0/629.95**	4.0/645.3894	4.0/645.3894	6.18	4.0/629.95
c203	**4.0/629.95**	4.0/643.4462	4.0/643.4462	7.30	4.0/629.95
c204	**4.0/629.95**	4.0/636.43	4.0/636.43	7.60	4.0/629.95
c205	**4.0/629.95**	4.0/638.1712	4.0/638.1712	6.46	4.0/629.95
c206	**4.0/629.95**	4.0/635.3832	4.0/635.3832	5.73	4.0/629.95
c207	**4.0/629.95**	4.0/632.7976	4.0/632.7976	6.27	4.0/629.95
c208	**4.0/629.95**	4.0/638.1712	4.0/638.1712	6.41	4.0/629.95
r101	18.0/1661.33	18.0/1630.135	**18.0/1630.135**	10.36	18.0/1661.33
r102	16.0/1461.48	15.0/1521.325	**15.0/1521.325**	10.26	16.0/1461.48
r103	**13.0/1262.75**	13.0/1264.807	13.0/1264.807	7.77	13.0/1262.75
r104	**11.0/1078.99**	11.0/1089.919	11.0/1089.919	12.87	11.0/1078.99
r105	15.0/1373.94	14.0/1396.798	**14.0/1396.798**	9.57	15.0/1373.94
r106	13.0/1310.46	13.0/1281.087	**13.0/1281.087**	9.69	13.0/1310.46
r107	**12.0/1118.91**	12.0/1127.709	12.0/1127.709	15.67	12.0/1118.91
r108	**11.0/1031.14**	11.0/1042.797	11.0/1042.797	17.69	11.0/1031.14
r109	13.0/1201.04	12.0/1265.818	**12.0/1265.818**	15.04	13.0/1201.04
r110	11.0/1112.8	11.0/1094.995	**11.0/1094.995**	11.31	11.0/1112.8
r111	12.0/1084.13	11.0/1147.225	**11.0/1147.225**	17.95	12.0/1084.13
r112	11.0/1017.31	11.0/1013.945	**11.0/1013.945**	7.68	11.0/1017.31
r201	3.0/1266.06	3.0/1261.637	3.0/1261.637	8.41	3.0/1258.39
r202	3.0/1052.32	3.0/1051.457	**3.0/1051.457**	9.93	3.0/1052.32
r203	**3.0/895.54**	3.0/900.6014	3.0/900.6014	10.79	3.0/895.54
r204	**2.0/780.14**	2.0/783.5278	2.0/783.5278	15.76	2.0/780.14
r205	**3.0/987.36**	3.0/987.362	3.0/987.362	9.47	3.0/987.36
r206	**3.0/922.7**	3.0/924.4825	3.0/924.4825	11.25	3.0/922.7
r207	2.0/846.59	2.0/846.5337	**2.0/846.5337**	15.69	2.0/846.59
r208	**2.0/736.12**	2.0/736.6421	2.0/736.6421	16.08	2.0/736.12
r209	3.0/868.95	3.0/867.7957	**3.0/867.7957**	10.83	3.0/868.95
r210	**3.0/843.36**	3.0/845.2673	3.0/845.2673	10.72	3.0/843.36
r211	2.0/862.56	2.0/857.1001	**2.0/857.1001**	19.61	2.0/862.56
rc101	16.0/1684.84	15.0/1725.727	**15.0/1725.727**	7.01	16.0/1684.84
rc102	14.0/1555.9	14.0/1540.257	**14.0/1540.257**	9.26	14.0/1555.9
rc103	13.0/1329.58	12.0/1388.715	**12.0/1388.715**	8.99	13.0/1329.58
rc104	11.0/1202.93	11.0/1181.263	**11.0/1181.263**	12.62	11.0/1202.93
rc105	**14.0/1458.49**	14.0/1463.486	14.0/1463.486	14.10	14.0/1458.49
rc106	13.0/1422.96	13.0/1397.55	**13.0/1397.55**	12.25	13.0/1422.96
rc107	12.0/1261.03	12.0/1255.031	**12.0/1255.031**	14.99	12.0/1261.03
rc108	11.0/1185.68	11.0/1165.596	**11.0/1165.596**	11.48	11.0/1185.68
rc201	4.0/1446.84	4.0/1446.032	**4.0/1446.032**	7.04	4.0/1446.84
rc202	**3.0/1416.96**	3.0/1434.175	3.0/1434.175	11.08	3.0/1416.96
rc203	3.0/1069.27	3.0/1061.117	**3.0/1061.117**	10.21	3.0/1069.27
rc204	3.0/887.76	3.0/887.1029	**3.0/887.1029**	12.19	3.0/887.76
rc205	**3.0/1262.22**	3.0/1289.078	3.0/1289.078	10.24	3.0/1262.22
rc206	3.0/1213.89	3.0/1200.743	**3.0/1200.743**	9.89	3.0/1213.89
rc207	3.0/993.49	3.0/985.6748	**3.0/985.6748**	11.83	3.0/993.49
rc208	3.0/839.71	3.0/836.9279	**3.0/836.9279**	13.33	3.0/839.71
Time	16.77 min			9.96	
Gap	0.0/0.01	0.5/0.20	-0.9/0.43		

Table 4.8: Comparison with the results for the E-VRPTWPR of Keskin & Çatay (2016).

4.7. Performance Analysis – E-FSMFTW

The E-FSMFTW is a closely related problem that considers a heterogeneous fleet of pure-electric vehicles and uses a fixed recharging scheme (always to maximum capacity). The instances are based on the previously mentioned E-VRPTW instances (Schneider et al., 2014) combined with the vehicle type definition for the FSMF (Liu & Shen, 1999). However, this type definition is extended by a varying battery capacity but a

shared consumption rate.

Type		HPRH Best 10	HPRH Avg 10	HPRH T(min)	Montoya Best 10	Montoya Avg 10	Montoya T(min)	HGA Best 10	HGA Avg 10	HGA T(min)
A	c	6470.08	6487.28	29.37	6464.93	6477.48	28.48	**6458.64**	**6462.47**	**19.62**
	r	3646.66	3673.97	30.05	3660.94	3676.95	21.95	**3616.28**	**3624.99**	**20.34**
	rc	4600.30	4639.24	**15.48**	4602.54	4621.68	27.67	**4579.84**	**4591.86**	17.92
B	c	2100.85	2114.16	25.21	2102.16	2109.79	25.85	**2097.43**	**2098.83**	**17.16**
	r	1623.81	1643.92	22.02	1658.11	1667.44	21.55	**1617.04**	**1627.26**	**15.23**
	rc	1933.33	1955.53	16.72	1966.50	1997.52	18.41	**1924.03**	**1935.08**	**12.54**
C	c	1495.12	1503.53	22.86	1498.40	1505.52	19.57	**1493.69**	**1494.53**	**12.47**
	r	1349.89	1368.57	21.92	1382.08	1391.79	34.42	**1344.26**	**1352.69**	**14.76**
	rc	1576.43	1594.96	17.26	1599.57	1612.44	28.02	**1570.55**	**1579.03**	**13.16**

Table 4.9: Comparison with heuristics from the literature for the E-FSMFTW. HPRH: Hiermann et al. (2016); Montoya (2016)

Table 4.9 shows the results for the E-FSMF benchmark instances. The results are grouped by vehicle type (A,B,C), and we report the average values for each instance type (c,r,rc). For the ALNS of Hiermann et al. (2016) (HPRH), the parallel matheuristic of Montoya (2016), and our HGA, we report (a) the best objective value, (b) the average over 10 runs, and (c) the average CPU time in minutes. HGA performs very well compared to the other algorithms, finding better results on average for all instance-type combination. The time over all instances is 15.80 min for the HGA, which compares well with 22.66 min (HPRH) and 25.20 min (Montoya).

Detailed results are presented in the Appendix. Our algorithm found 119 new best solutions for the 168 instances in the benchmark set.

5. Conclusions

In this paper, we have introduced an vehicle routing problem variant considering a mix of conventional, hybrid, and electric vehicles. The study of this prototypical problem allow to better understand how to compose and route a fleet of vehicles with different properties and different constraints, and to study the relative role of each vehicle in operational settings. This problem bridges the gap between the classical VRP and the electric VRP, and includes possible plug-in hybrid vehicles which form an intermediate option between the two types of propulsion.

To solve this problem, we have introduced an efficient hybrid genetic algorithm. We implemented a layered route evaluation approach to solve the subproblems, therefore decomposing the problem into a pure assignment and sequencing problem, in the top layer, and problem-specific route evaluations in a bottom layer. We use a set of labeling and greedy evaluation methods to find an optimal placement of recharging stations visits and select the propulsion mode over the trip for hybrid vehicles. The efficiency of the method is demonstrated on a variety of benchmark instances of the related E-FSMF and the E-VRPTW variants. As illustrated by our computational results, the method produced average solutions of equal or higher quality than existing algorithms for these problems. It also found 119 new best solutions for the E-FSMF, 11 for the E-VRPTW and 19 for the E-VRPTWPR.

Our computational studies also show the relevance of this broader problem formulation and provide insights into various managerial implications. In particular, we considered different fuel and energy price scenarios to observe their impact on the optimized fleet mix. Our results show that the operational cost of the best mixed fleet can be 7% lower than the best homogeneous fleet with either ICEV, BEV or PHEV. Therefore, logistic activities in the coming decades may require a mix of vehicles and propulsion types to achieve competitiveness. Furthermore, even if hybrid plug-in vehicles tend to consume more energy than fully electric vehicle due to their heavier base load, our experiments confirm that their ability to switch fuel on a trip can help cutting down operational costs. PHEV do not usually represent the majority of the vehicles in our optimized solutions, but a few hybrid vehicles are recurrent in a majority of scenarios with intermediate fuel and energy price.

To stimulate further research, we make available a new benchmark set for the based on the classical electric VRP and vehicle parameters from real-world data.[1] As a next step we will add additional real-world constraints in the form of city-center restrictions. These restrictions prohibit or penalize the use of ICEVs in specified areas, as is the case in several cities around the world. This will provide an insight into the fleet needed for cost-efficient operation in urban areas. We will also further explore the systematic evaluation methodology and its use for other VRP classes.

Acknowledgments

We wish to thank our colleagues at the Austrian Institute of Technology and the University of Vienna as well as the participants of various conferences for useful discussions and suggestions. This work is partially funded by the Austrian Climate and Energy Fund within the Electric Mobility Flagship Projects program under grant 834868 (project VECEPT). This support is gratefully acknowledged.

References

Abdallah, T. (2013). *The Plug-In Hybrid Electric Vehicle Routing Problem with Time Windows*. Master's thesis University of Waterloo Canada.

AustriaTech (2014). Annex: Electric fleets in urban logistics, project ENCLOSE. Last accessed 2015-07-21.

Baldacci, R., Battarra, M., & Vigo, D. (2008). Routing a heterogeneous fleet of vehicles. In B. Golden, S. Raghavan, & E. Wasil (Eds.), *The Vehicle Routing Problem: Latest Advances and New Challenges* (pp. 3–27). New York, NY, USA: Springer US volume 43 of *Operations Research/Computer Science Interfaces*.

Christiaens, J., & Vanden Berghe, G. (2016). *A fresh ruin & recreate implementation for the capacitated vehicle routing problem*. Technical Report KU Leuven Ghent, Belgium.

Conrad, R. G., & Figliozzi, M. A. (2011). The recharging vehicle routing problem. In T. Doolen, & E. Van Aken (Eds.), *Proceedings of the 2011 Industrial Engineering Research Conference*. Reno, NV, USA.

Desaulniers, G., Errico, F., Irnich, S., & Schneider, M. (2016). Exact algorithms for electric vehicle-routing problems with time windows. *Operations Research*, *64*, 1388–1405.

Edenhofer, O., Pichs-Madruga, R., Sokona, Y., Minx, J. C., Farahani, E., Kadner, K., S. Seyboth, Adler, A., Baum, I., Brunner, S., Eickemeier, P., Kriemann, B., Savolainen, J., Schlömer, S., Von Stechow, C., & Zwickel, T. (Eds.) (2014). *Climate Change 2014: Mitigation of Climate Change. Working Group III Contribution to the Fifth Assessment Report of the Intergovernmental Panel on Climate Change*. New York, NY, USA: Cambridge University Press.

Erdoğan, S., & Miller-Hooks, E. (2012). A green vehicle routing problem. *Transportation Research Part E: Logistics and Transportation Review*, *48*, 100–114.

Felipe, A., Ortuño, M. T., Righini, G., & Tirado, G. (2014). A heuristic approach for the green vehicle routing problem with multiple technologies and partial recharges. *Transportation Research Part E: Logistics and Transportation Review*, *71*, 111–128.

Garaix, T., Artigues, C., Feillet, D., & Josselin, D. (2010). Vehicle routing problems with alternative paths: An application to on-demand transportation. *European Journal of Operational Research*, *204*, 62–75.

Goeke, D., & Schneider, M. (2015). Routing a mixed fleet of electric and conventional vehicles. *European Journal of Operational Research*, *245*, 81–99.

[1] `http://www.vrp-rep.org/datasets/item/2017-0029.html`

Goel, A., & Vidal, T. (2014). Hours of service regulations in road freight transport: An optimization-based international assessment. *Transportation Science*, *48*, 391–412.

Hiermann, G., Puchinger, J., & Hartl, R. F. (2014). The electric fleet size and mix vehicle routing problem with time windows and recharging stations. Working paper March 2014, University of Vienna, Austria.

Hiermann, G., Puchinger, J., Ropke, S., & Hartl, R. F. (2016). The electric fleet size and mix vehicle routing problem with time windows and recharging stations. *European Journal of Operational Research*, *252*, 995–1018.

Irnich, S., & Desaulniers, G. (2005). Shortest path problems with resource constraints. In G. Desaulniers, J. Desrosiers, & M. M. Solomon (Eds.), *Column Generation* (pp. 33–65). New York, NY, USA: Springer US.

Irnich, S., & Villeneuve, D. (2006). The shortest-path problem with resource constraints and k-cycle elimination for k $\geq$ 3. *INFORMS Journal on Computing*, *18*, 391–406.

Keskin, M., & Çatay, B. (2016). Partial recharge strategies for the electric vehicle routing problem with time windows. *Transportation Research Part C: Emerging Technologies*, *65*, 111–127.

Lebeau, P., De Cauwer, C., Van Mierlo, J., Macharis, C., Verbeke, W., & Coosemans, T. (2015). Conventional, hybrid, or electric vehicles: Which technology for an urban distribution centre? *The Scientific World Journal*, *2015*.

Liu, F.-H., & Shen, S.-Y. (1999). The fleet size and mix vehicle routing problem with time windows. *Journal of the Operational Research Society*, *50*, 721–732.

Montoya, J.-A. (2016). *Electric Vehicle Routing Problems: Models and solution approaches*. Ph.D. thesis Université d'Angers France.

Nagata, Y., Bräysy, O., & Dullaert, W. (2010). A penalty-based edge assembly memetic algorithm for the vehicle routing problem with time windows. *Computers & Operations Research*, *37*, 724–737.

Pelletier, S., Jabali, O., & Laporte, G. (2016). Goods distribution with electric vehicles: Review and research perspectives (50th anniversary invited article). *Transportation Science*, *50*, 3–22.

Plötz, P., Gnann, T., Wietschel, M., & Kühn, A. (2013). Markthochlaufszenarien für elektrofahrzeuge - langfassung, Fraunhofer ISI, Karlsruhe. Last accessed 2016-04-01.

Prins, C. (2004). A simple and effective evolutionary algorithm for the vehicle routing problem. *Computers & Operations Research*, *31*, 1985–2002.

Prins, C. (2009). Two memetic algorithms for heterogeneous fleet vehicle routing problems. *Engineering Applications of Artificial Intelligence*, *33*, 916–928.

Ropke, S., & Pisinger, D. (2006). An adaptive large neighborhood search heuristic for the pickup and delivery problem with time windows. *Transportation Science*, *40*, 455–472.

Sassi, O., Cherif-Khettaf, W. R., & Oulamara, A. (2015). Vehicle routing problem with mixed fleet of conventional and heterogenous electric vehicles and time dependent charging costs. *International Journal of Mathematical, Computational, Physical, Electrical and Computer Engineering*, *9*, 171–181.

Schneider, M., Stenger, A., & Goeke, D. (2014). The electric vehicle routing problem with time windows and recharging stations. *Transportation Science*, *48*, 500–520.

Subramanian, A., Uchoa, E., & Ochi, L. S. (2013). A hybrid algorithm for a class of vehicle routing problems. *Computers & Operations Research*, *40*, 2519–2531.

Toth, P., & Vigo, D. (2014). *Vehicle Routing: Problems, Methods, and Applications, Second Edition*. Philadelphia, PA, USA: Society for Industrial and Applied Mathematics.

Vidal, T. (2017). Node, edge, arc routing and turn penalties : Multiple problems – One neighborhood extension. *Operations Research*, *65*, 992–1010.

Vidal, T., Crainic, T. G., Gendreau, M., Lahrichi, N., & Rei, W. (2012). A hybrid genetic algorithm for multidepot and periodic vehicle routing problems. *Operations Research*, *60*, 611–624.

Vidal, T., Crainic, T. G., Gendreau, M., & Prins, C. (2013). A hybrid genetic algorithm with adaptive diversity management for a large class of vehicle routing problems with time-windows. *Computers & Operations Research*, *40*, 475–489.

Vidal, T., Crainic, T. G., Gendreau, M., & Prins, C. (2015a). Time-window relaxations in vehicle routing heuristics. *Journal of Heuristics*, *21*, 329–358.

Vidal, T., Crainic, T. G., Gendreau, M., & Prins, C. (2015b). Timing problems and algorithms: Time decisions for sequences of activities. *Networks*, *65*, 102–128.

Zündorf, T. (2014). *Electric Vehicle Routing with Realistic Recharging Models*. Master's thesis Karlsruhe Institute of Technology Germany.

Appendix A. Appendix

Appendix A.1. Greedy charging policy for PHEVs

In Section 3.1.1, we described the extension functions for evaluating the routes of PHEVs. We outlined the key steps of the greedy policy required to ensure that the cost of the route is minimal without violating the time and energy constraints. In summary, these are: 1) use electric energy mode first, since we assume that electricity is cheaper than fossil fuel; 2–3) recharge only when necessary or to avoid waiting time, to minimize costs while ensuring time-feasibility similar to that for BEVs; and 4) revert recharging operations only if time windows are violated, to ensure that fossil fuel is used only when necessary.

As for the BEV extension function, we define the following resource extension functions, denoted T_i^{res}. The intermediate calculations, starting with Δ, are described along with the functions.

$$T_j^{\mathrm{DIST}} = T_i^{\mathrm{DIST}} + d_{ij} \tag{A.1}$$
$$T_j^{\mathrm{Q}} = T_i^{\mathrm{Q}} + q_j \tag{A.2}$$

The distance and capacity resources are T_i^{DIST} and T_i^{Q}. Their respective extensions simply add the distance traveled or the additional load.

$$T_j^{\mathrm{DUR^F}} = T_i^{\mathrm{DUR^F}} + t_{ij} + s_j + \Delta^{\mathrm{WT^F}} \tag{A.3}$$
$$T_j^{\mathrm{TW}} = T_i^{\mathrm{TW}} + \Delta^{\mathrm{TW^F}} \tag{A.4}$$
$$\Delta^{\mathrm{DUR^F}} = T_i^{\mathrm{DUR^F}} - T_i^{\mathrm{TW}} + t_{ij} \tag{A.5}$$
$$\Delta^{\mathrm{WT^F}} = \max\{e_j - \Delta^{\mathrm{DUR^F}} - e_0, 0\} \tag{A.6}$$
$$\Delta^{\mathrm{TW^F}} = \max\{e_0 + \Delta^{\mathrm{DUR^F}} - l_j, 0\} \tag{A.7}$$

According to our formulation, PHEVs can use either the electric engine or the ICE. The use of the electric energy stored in the battery may require a reloading operation, which takes time. This could lead to a violation of the time constraint. Equation (A.3) calculates the duration of the route if only the ICE is used; this is the minimal duration for this route. Time-window violations can be repaired only by reverting a recharging operation to this lower bound. Any further violation is penalized using a time warp, as described in Section 3.1.1 for BEVs. Using the intermediate calculations (A.5)–(A.7), the additional time warp is computed in Equation (A.4).

$$T_j^{\mathrm{DUR}} = T_i^{\mathrm{DUR}} + t_{ij} + s_j + \Delta^{\mathrm{WT}} + \overrightarrow{\Delta}^{\mathrm{T^{RC}}} - \Delta^{\mathrm{T^{ADJ}}} \tag{A.8}$$
$$T_j^{\mathrm{DIST^F}} = T_i^{\mathrm{DIST^F}} + (\Delta^{\mathrm{EY^{RC}}} + \Delta^{\mathrm{T^{ADJ}}}/g)/r_{\mathrm{E}} \tag{A.9}$$
$$\overrightarrow{\Delta}^{\mathrm{Y^{RC}}} = \max\{\min\{d_{ij} \cdot r_{\mathrm{E}} - T_i^{\mathrm{Y}}, T_i^{\mathrm{YAR}}, T_i^{\mathrm{TAR}}/g\}, 0\} \tag{A.10}$$
$$\overrightarrow{\Delta}^{\mathrm{T^{RC}}} = \overrightarrow{\Delta}^{\mathrm{Y^{RC}}} \cdot g \tag{A.11}$$
$$\Delta = T_i^{\mathrm{DUR}} + \overrightarrow{\Delta}^{\mathrm{Y^{RC}}} \cdot g - T_i^{\mathrm{TW}} + t_{ij} \tag{A.12}$$
$$\Delta^{\mathrm{EY^{RC}}} = \max\{T_i^{\mathrm{Y}} - d_{ij} \cdot r_{\mathrm{E}} - \overrightarrow{\Delta}^{\mathrm{Y^{RC}}}, 0\} \tag{A.13}$$
$$\Delta^{\mathrm{TW}} = \max\{e_0 + \Delta - l_j, 0\} \tag{A.14}$$
$$\Delta^{\mathrm{T^{ADJ}}} = \max\{\Delta^{\mathrm{TW}} - \Delta^{\mathrm{TW^F}}, 0\} \tag{A.15}$$
$$\Delta^{\mathrm{WT}} = \max\{e_j - (\Delta - \Delta^{\mathrm{T^{ADJ}}}) - e_0, 0\} \tag{A.16}$$

Equation (A.8) calculates the duration of the route after vertex j based on the travel time (t_{ij}), service time (s_j), waiting time (Δ^{WT}), and PHEV-specific calculations. These consist of two terms: a) the recharging time at the last recharging station visited before vertex j ($\overrightarrow{\Delta}^{\mathrm{T^{RC}}}$), and b) the time gained by using fuel instead of electric energy ($\Delta^{\mathrm{T^{ADJ}}}$). Similarly to the BEV case, we recharge only when necessary. However, we can avoid

time-window violations by choosing not to recharge. Equation (A.10) uses the minimum energy required to recharge, the amount available to recharge based on the energy restriction, and the time available. If the amount of electric energy required does not exceed the current energy level, the first term will be negative and the equation evaluates to zero. The duration until arrival at vertex j is calculated in Equation (A.12), which adds the time required to recharge ($\overrightarrow{\Delta}^{\mathrm{Y^{RC}}} \cdot g$) to the travel time minus the previous time warp. With this, we can calculate the lateness and thus the time warp required when recharging (A.14). However, as stated previously, we can avoid time warp by using fuel instead of electric energy, and our policy enforces this behavior. Equation (A.15) is used to calculate the repairable time warp, which is the difference between the time warp with and without recharging operations. This value has to be removed from the duration when calculating the waiting time (see A.16).

The second equation in this listing (A.9) calculates the distance traveled using fuel instead of electric energy. This value is increased by summing the energy that is not rechargeable ($\Delta^{\mathrm{EY^{RC}}}$) and the electric energy traded for fuel to avoid time warp ($\Delta^{\mathrm{T^{ADJ}}}/g$) divided by the electric energy consumption (r_{E}) to get the distance value.

$$T_j^{\mathrm{YAR}} = \begin{cases} Y - \Delta^{\mathrm{Y^{RC}}} & \text{if } j \in \mathcal{F} \\ \Delta^{\mathrm{YAR}} & \text{otherwise} \end{cases} \tag{A.17}$$

$$T_j^{\mathrm{TAR}} = \min\{\max\{0, l_j - e_0 - T_j^{\mathrm{DUR}} + T_j^{\mathrm{TW}}\}, \Delta^{\mathrm{TAR}}\} \tag{A.18}$$

$$T_j^{\mathrm{Y}} = T_i^{\mathrm{Y}} - d_{ij} \cdot r_{\mathrm{E}} + \Delta^{\mathrm{Y^{RC}}} \tag{A.19}$$

$$\Delta^{\mathrm{YAR}} = \begin{cases} 0 & \text{if } \Delta^{\mathrm{T^{ADJ}}} > 0 \\ T_i^{\mathrm{YAR}} - \overrightarrow{\Delta}^{\mathrm{Y^{RC}}} & \text{otherwise} \end{cases} \tag{A.20}$$

$$\Delta^{\mathrm{TAR}} = \begin{cases} +\infty & \text{if } j \in \mathcal{F} \\ T_i^{\mathrm{TAR}} - \overrightarrow{\Delta}^{\mathrm{Y^{RC}}} \cdot g & \text{otherwise} \end{cases} \tag{A.21}$$

$$\Delta^{\mathrm{Y^{RC}}} = \overrightarrow{\Delta}^{\mathrm{Y^{RC}}} + \min\{\Delta^{\mathrm{WT}}/g, \Delta^{\mathrm{YAR}}\} \tag{A.22}$$

To keep track of the amount of energy we can recharge, we use two resources: the amount of rechargeable energy (T^{YAR}) and the time available to recharge (T^{TAR}). The first value is updated by calculating the total amount of energy recharged to this point (A.22). When we extend to a recharging station, the previous state plus the amount recharged define the value. Otherwise, we have to differentiate between the two cases described in (A.20): a) time adjustment ($\Delta^{\mathrm{T^{ADJ}}} > 0$), which will set the rechargeable amount to zero because we have to reverse earlier recharging decisions, so no additional recharging is viable; and b) no adjustment, so we reduce the possible amount by the amount we have already recharged.

The second resource (time available to recharge) is updated using Equation (A.18). This finds the minimum of a) the maximum, non-negative available time in the vertex and b) either the previous available time minus the recharging time for the current vertex ($\overrightarrow{\Delta}^{\mathrm{Y^{RC}}}$), or infinity if the current vertex is a recharging station.

Using these extension functions we can define the objective function as follows:

$$T_j^{cost} = T_j^{\mathrm{DIST}} \cdot r_{\mathrm{E}} \cdot c_{\mathrm{E}} + T_j^{\mathrm{DIST^F}} \cdot r_{\mathrm{F}} \cdot c_{\mathrm{F}} \tag{A.23}$$

Appendix A.2. Labeling for PHEVs

The resources for the PHEV labeling are:

$$R^{\mathrm{PHEV}} = \{v, T^{\mathrm{COST}}(), T^{\mathrm{DUR}}(), T^{\mathrm{DUR^F}}(), T^{\mathrm{Y}}(), T^{\mathrm{YAR}}(), T^{\mathrm{TAR}}()\}$$

where $T^{\mathrm{COST}}(L)$ is the cost of the label, $T^{\mathrm{DUR}}(L)$ the time duration at $v(L)$, $T^{\mathrm{DUR^F}}(L)$ time duration without recharging, and $T^{\mathrm{Y}}(L)$ the current energy level. $T^{\mathrm{YAR}}(L)$ is the rechargeable energy and $T^{\mathrm{TAR}}(L)$ the maximum

recharging time, both at the last recharging station visited. These values are taken directly from the result of the evaluation methods described above.

$$T^{\text{COST}}(L_1) \leq T^{\text{COST}}(L_2) \tag{A.24}$$
$$T^{\text{DUR}}(L_1) \leq T^{\text{DUR}}(L_2) \tag{A.25}$$
$$T^{\text{DUR}^{\text{F}}}(L_1) \leq T^{\text{DUR}^{\text{F}}}(L_2) \tag{A.26}$$
$$T^{\text{Y}}(L_1) \geq T^{\text{Y}}(L_2) \tag{A.27}$$
$$T^{\text{Y}}(L_1) + T^{\text{YAR}}(L_1)' \geq T^{\text{Y}}(L_2) + T^{\text{YAR}}(L_2)' \tag{A.28}$$

The dominance criterion is defined as follows: A label L_1 dominates L_2 if the cost (A.24), the duration with recharging (A.25), and the duration without recharging (A.25) are less than the values for L_2, and the current (A.27) and the maximum available energy (A.28) are greater than the vaues for L_2.

This simple criterion is similar to that defined for BEVs in Section 3.1.2. It adds a check for the time without recharging, because we could avoid recharging by using the ICE. This prevents the removal of labels that are potentially costly but could fulfill customer time-window restrictions. Clearly, this will increase the number of labels we have to consider and thus impact the overall CPU time. To strengthen the criterion and allow for a more aggressive removal of labels, we define a stricter criterion as follows:

$$T^{\text{COST}}(L_1) \leq T^{\text{COST}}(L_2) \tag{A.29}$$
$$T^{\text{DUR}^{\text{F}}}(L_1) \leq T^{\text{DUR}^{\text{F}}}(L_2) \tag{A.30}$$

$$\begin{gathered} T^{\text{DUR}}(L_1) \leq T^{\text{DUR}}(L_2) \vee \\ (T^{\text{DUR}}(L_1) - T^{\text{DUR}^{\text{F}}}(L_1) \geq T^{\text{DUR}}_{1-2} \ \wedge \ T^{\text{DUR}}(L_1) + \rho(T^{\text{DUR}}_{1-2}/g) \leq T^{\text{COST}}(L_2)) \end{gathered} \tag{A.31}$$

$$\begin{gathered} T^{\text{Y}}(L_1) + T^{\text{YAR}}(L_1)' \geq T^{\text{Y}}(L_2) + T^{\text{YAR}}(L_2)' \vee \\ \begin{pmatrix} (T^{\text{DUR}}(L_1) - T^{\text{DUR}^{\text{F}}}(L_1)) \cdot g \geq T^{\text{Y}}_{2-1} \wedge \\ T^{\text{COST}}(L_1) + \rho(T^{\text{Y}}_{2-1}) \leq T^{\text{COST}}(L_2) \end{pmatrix} \end{gathered} \tag{A.32}$$

$$\begin{gathered} T^{\text{Y}}(L_1) \geq T^{\text{Y}}(L_2) \vee \\ \begin{pmatrix} (T^{\text{DUR}}(L_1) - T^{\text{DUR}^{\text{F}}}(L_1)) \cdot g \geq T^{\text{Y}}_{2-1} + T^{\text{YAR}}_{2-1} \wedge \\ T^{\text{COST}}(L_1) + \rho(T^{\text{Y}}_{2-1} + T^{\text{YAR}}_{2-1}) \leq T^{\text{COST}}(L_2) \end{pmatrix} \end{gathered} \tag{A.33}$$

where

$$T^{\text{YAR}}(L_i)' = \min\{T^{\text{YAR}}(L_i), T^{\text{TAR}}(L_i) \cdot g\} \tag{A.34}$$
$$T^{\text{RES}}_{i-j} = T^{\text{RES}}(L_i) - T^{\text{RES}}(L_j) \tag{A.35}$$
$$\rho(y) = y/c_{\text{E}} \cdot c_{\text{F}} \tag{A.36}$$

Equations (A.29) and (A.30) are the same as before, comparing the cost and time without electric energy. Equation (A.31) extends and replaces Equation (A.25) by taking into account the possibility of avoiding recharging times by using the ICE. The first part, as before, checks whether the duration of L_1 is lower than L_2. If it is not, a second check tests whether enough time can be reversed; if so, label L_1 has a still lower cost after the update. Equations (A.32) and (A.33) are defined similarly. If the total amount of electric energy available (or current electric energy available, respectively) of L_1 is less than L_2, then again the reversible

amount is checked. If it is possible to reverse enough energy usage, the cost is again compared with the additional cost of using fossil fuel instead of electric energy.

Appendix A.3. Detailed results for the E-FSMF

Tables A.1, A.2 and A.3 show the results for the E-FSMF instance set. For the ALNS of Hiermann et al. (2016) (HPRH), the parallel matheuristic of Montoya (2016), and our HGA, we report the average, and the best objective value over 10 runs, as well as the average CPU time in minutes.

A		**HPRH**			**Montoya**			**HGA**		**BKS**
Name	Avg 10	Best 10	T(min)	Avg 10	Best 10	T(min)	Avg 10	Best 10	T(min)	
c101	7190.21	7180.42	**17.53**	7165.15	7162.01	25.88	**7162.29**	**7160.77**	21.12	7162.01
c102	7162.24	7154.50	**17.95**	7142.80	7139.45	26.02	**7141.25**	**7137.04**	21.86	7139.45
c103	7149.31	7126.29	**18.30**	7124.26	7121.12	31.22	**7122.27**	**7117.32**	22.93	7121.12
c104	7110.43	7100.22	**17.75**	7103.79	7099.88	32.93	**7098.38**	**7097.80**	23.99	7099.88
c105	7182.56	7155.23	**17.60**	**7152.21**	7140.31	27.24	7156.31	**7138.85**	21.15	7140.31
c106	7168.94	7146.88	**17.69**	7141.66	7136.90	27.28	**7140.15**	**7134.75**	21.92	7136.90
c107	7171.04	7156.18	**17.42**	7145.54	7139.12	30.49	**7142.77**	**7136.44**	21.24	7139.12
c108	7153.77	7141.49	**17.53**	7142.39	7133.30	30.22	**7139.50**	**7131.83**	21.99	7133.30
c109	7132.19	7120.33	**17.32**	7132.66	7123.15	33.32	**7120.07**	**7113.94**	22.39	7120.33
c201	5757.53	5737.57	39.28	5741.28	5736.35	19.36	**5738.23**	**5736.11**	**13.72**	5736.35
c202	5765.52	5744.65	42.22	5753.56	5740.43	21.50	**5735.61**	**5733.53**	**15.76**	5740.43
c203	5751.99	5726.08	47.69	5783.33	5744.25	28.27	**5713.38**	**5713.38**	**18.73**	5726.08
c204	5727.18	5705.82	50.91	5772.72	5724.75	41.49	**5691.37**	**5689.04**	**21.21**	5705.82
c205	5725.41	5703.48	46.16	5701.83	5694.58	24.43	**5696.48**	**5693.45**	**15.21**	5694.58
c206	5714.39	5708.77	31.20	5696.99	5689.08	26.40	**5687.96**	**5687.96**	**16.90**	5689.08
c207	5713.44	5697.99	32.58	5716.37	5696.54	27.61	**5694.47**	**5693.23**	**17.30**	5696.54
c208	5707.65	5685.40	50.23	5700.58	5682.60	30.48	**5681.47**	**5681.47**	**16.10**	5682.60
r101	4465.51	4426.85	14.47	**4379.64**	**4366.21**	21.41	4382.32	4372.29	**9.12**	4366.21
r102	4270.92	4245.82	14.97	**4180.61**	**4176.82**	13.11	4202.05	4186.74	**10.06**	4176.82
r103	4130.86	4103.35	16.43	**4049.01**	**4043.29**	15.53	4060.29	4048.37	**11.82**	4043.29
r104	4025.60	4007.28	15.27	**3970.77**	3969.12	21.45	3972.91	**3966.74**	**13.77**	3969.12
r105	4215.34	4181.80	15.37	**4140.08**	**4138.01**	12.94	4154.04	4145.27	**9.51**	4138.01
r106	4155.24	4120.23	15.54	**4075.44**	**4068.15**	16.46	4087.59	4078.17	**11.22**	4068.15
r107	4093.59	4057.06	15.30	**4008.71**	4003.84	24.07	4011.87	**4000.69**	**12.26**	4003.84
r108	4025.75	3992.57	**15.77**	**3961.93**	**3955.48**	23.96	3968.72	3961.92	17.29	3955.48
r109	4110.98	4067.14	15.58	**4024.49**	**4016.33**	19.92	4034.36	4023.64	**11.85**	4016.33
r110	4045.96	4024.71	**15.73**	**3975.95**	**3969.02**	26.51	3991.65	3973.72	16.88	3969.02
r111	4048.42	4023.38	**15.93**	**3976.91**	**3972.84**	25.10	3990.36	3984.77	16.66	3972.84
r112	4023.01	4001.87	**15.80**	**3947.93**	3942.68	21.85	3955.19	**3942.66**	16.23	3942.68
r201	3432.83	3413.93	42.20	3543.81	3515.45	17.91	**3410.53**	**3399.82**	**17.61**	3413.93
r202	3295.26	3270.49	44.95	3397.33	3366.13	**18.23**	**3275.73**	**3266.47**	20.93	3270.49
r203	3169.97	3136.47	49.40	3252.78	3224.34	**23.86**	**3137.34**	**3127.56**	24.10	3136.47
r204	3026.09	3008.01	46.32	3114.40	3098.94	**26.84**	**3003.15**	**3002.72**	29.11	3008.01
r205	3261.16	3234.26	40.89	3356.01	3326.29	21.28	**3240.34**	**3230.20**	**20.48**	3234.26
r206	3194.12	3172.50	47.73	3296.06	3261.05	26.25	**3161.18**	**3156.58**	**22.96**	3172.50
r207	3099.52	3079.39	46.87	3175.13	3159.76	**23.25**	**3062.33**	**3059.85**	28.94	3079.39
r208	3026.57	3010.51	51.26	3104.77	3088.29	**33.89**	**2999.40**	**2995.96**	34.17	3010.51
r209	3161.57	3142.72	45.06	3255.62	3224.28	25.29	**3133.33**	**3122.41**	**23.40**	3142.72
r210	3143.79	3110.90	45.94	3235.09	3181.95	25.02	**3109.03**	**3101.10**	**22.95**	3110.90
r211	3079.24	3041.93	44.29	3147.32	3133.26	**20.83**	**3030.99**	**3026.74**	28.18	3041.93
rc101	5346.49	5294.01	14.13	**5255.03**	**5247.39**	13.21	5261.36	5254.50	**9.06**	5247.39
rc102	5180.03	5121.53	14.63	5118.29	5114.15	24.81	**5096.49**	**5069.43**	**10.34**	5114.15
rc103	5007.37	4958.51	14.53	**4924.38**	4916.98	18.60	4929.17	**4905.29**	**9.41**	4916.98
rc104	4862.65	4804.00	16.03	4815.22	4801.06	24.28	**4808.85**	**4783.16**	**10.50**	4801.06
rc105	5117.09	5074.43	14.48	5068.85	5060.96	14.74	**5063.17**	**5044.93**	**9.95**	5060.96
rc106	5102.46	5028.28	14.69	**5001.29**	**4985.03**	14.12	5002.07	4991.29	**9.97**	4985.03
rc107	4913.90	4864.78	15.24	**4853.96**	**4835.75**	15.67	4859.83	4836.81	**10.66**	4835.75
rc108	4862.41	4814.33	15.64	4819.12	**4798.48**	23.59	**4815.83**	4800.17	**10.25**	4798.48
rc201	4361.17	4346.25	**14.27**	4388.86	4371.85	32.88	**4343.47**	**4337.60**	21.58	4346.25
rc202	4295.27	4273.74	**14.59**	4313.51	4288.62	31.02	**4271.96**	**4267.75**	24.23	4273.74
rc203	4186.28	4152.94	**15.98**	4227.27	4191.76	36.69	**4152.79**	**4147.68**	26.63	4152.94
rc204	4127.11	4113.49	**19.18**	4160.55	4136.86	46.62	**4096.59**	**4094.11**	29.46	4113.49
rc205	4273.59	4246.52	**14.86**	4294.99	4274.33	33.33	**4248.30**	**4242.63**	23.58	4246.52
rc206	4270.25	4237.75	**15.09**	4289.85	4260.22	33.95	**4241.71**	**4236.43**	24.08	4237.75
rc207	4199.60	4177.23	**16.20**	4242.41	4215.09	36.42	**4174.39**	**4169.59**	26.14	4177.23
rc208	4122.12	4097.04	**18.13**	4173.32	4142.05	42.75	**4103.79**	**4096.01**	30.99	4097.04
Avg			25.68			25.57			18.75	
Gap	0.94	0.36		0.80	0.46		0.07	-0.10		

Table A.1: Comparison with the best known solutions for the E-FSMFTW, Type-A. BnP/HPRH: Hiermann et al. (2016); Montoya (2016).

B		**HPRH**			**Montoya**			**HGA**		**BKS**
Name	Avg 10	Best 10	T(min)	Avg 10	Best 10	T(min)	Avg 10	Best 10	T(min)	
c101	2505.73	2495.00	14.43	2502.09	**2495.00**	25.56	**2496.28**	**2495.00**	**13.59**	2495.00
c102	2450.73	2445.99	14.41	2451.39	2448.76	25.86	**2446.48**	**2445.99**	**13.85**	2445.99
c103	2452.40	2438.54	**15.03**	2437.99	2430.72	31.16	**2435.42**	**2427.44**	19.49	2430.72
c104	2428.95	2404.97	**15.07**	2410.12	2404.73	32.85	**2404.40**	**2402.47**	20.12	2404.73
c105	2475.95	2472.93	**14.45**	2476.46	2473.79	27.16	**2473.14**	**2472.60**	17.21	2472.93
c106	2468.13	2462.54	**14.71**	2466.25	2462.90	27.20	**2459.90**	**2456.74**	16.63	2462.54
c107	2461.32	2458.37	**14.60**	2459.31	2458.37	30.25	**2457.98**	**2457.89**	16.53	2458.37
c108	2463.02	2450.17	**14.33**	2455.74	2452.58	30.17	**2451.13**	**2448.08**	18.82	2450.17
c109	2452.57	2436.41	**15.07**	2434.02	2431.87	33.22	**2432.77**	**2431.36**	19.22	2431.87
c201	1739.26	1730.41	35.76	1730.50	**1730.41**	**14.14**	**1730.41**	**1730.41**	14.51	1730.41
c202	1745.24	1737.57	38.14	1730.12	**1729.73**	17.01	**1730.05**	**1729.73**	**16.40**	1729.73
c203	1742.76	1716.29	39.38	1743.23	1730.26	23.73	**1713.38**	**1713.38**	**18.46**	1716.29
c204	1709.43	1699.07	37.02	1753.55	1724.75	36.43	**1690.01**	**1689.04**	**21.42**	1699.07
c205	1715.09	1697.01	37.83	1701.83	1694.58	17.33	**1694.83**	**1693.45**	**15.38**	1694.58
c206	1712.38	1693.15	36.78	1696.99	1689.08	20.69	**1687.96**	**1687.96**	**16.68**	1689.08
c207	1710.70	1694.61	35.05	1715.61	1696.54	22.19	**1694.47**	**1693.23**	**16.92**	1694.61
c208	1707.11	**1681.47**	36.46	1701.29	1682.60	24.49	**1681.47**	**1681.47**	**16.56**	1681.47
r101	2281.28	2261.21	13.68	**2253.93**	2253.04	10.71	2258.24	2249.24	**7.75**	2249.14
r102	2095.87	2073.03	14.45	**2057.97**	2053.42	**8.01**	2063.58	**2047.89**	8.80	2047.89
r103	1927.52	1894.98	15.11	**1897.06**	**1892.84**	13.13	1906.46	1898.26	**9.50**	1892.84
r104	1775.33	**1747.65**	15.28	**1761.84**	1749.48	22.78	1766.32	1754.22	**10.63**	1747.65
r105	2030.12	2010.31	15.08	**2007.01**	1998.80	9.17	2013.63	2007.40	**8.79**	1997.75
r106	1963.88	1934.00	14.51	**1929.13**	1925.83	12.02	1948.02	**1925.56**	**9.52**	1925.83
r107	1844.20	1824.88	15.50	**1820.75**	**1818.03**	22.10	1842.49	1824.68	**10.21**	1818.03
r108	1753.09	1729.18	16.27	1733.87	1720.78	23.31	**1732.21**	**1712.40**	**10.93**	1720.78
r109	1904.12	1871.54	15.37	**1867.32**	1863.48	25.36	1877.84	**1861.15**	**9.75**	1863.48
r110	1793.48	1759.69	15.54	**1755.92**	**1752.40**	12.89	1786.94	1766.10	**10.67**	1752.40
r111	1808.36	1786.97	15.66	**1775.04**	**1765.08**	22.45	1793.86	1769.41	**10.62**	1765.08
r112	1746.02	1721.79	15.77	1722.34	1714.93	26.75	**1717.98**	**1705.89**	**10.74**	1714.93
r201	1618.25	1594.58	31.21	1714.30	1697.28	40.11	**1597.16**	**1591.35**	**14.57**	1594.58
r202	1479.42	1468.05	29.61	1551.73	1541.45	**17.87**	**1468.59**	**1461.63**	18.31	1468.05
r203	1354.24	1340.00	30.70	1438.89	1424.34	23.68	**1334.67**	**1327.56**	**20.54**	1340.00
r204	1211.63	1203.89	27.35	1286.75	1278.59	27.33	**1205.19**	**1202.72**	**26.38**	1203.89
r205	1455.08	1430.70	30.16	1534.24	1524.53	20.82	**1433.53**	**1429.32**	**17.53**	1430.70
r206	1376.34	1361.69	31.35	1470.36	1461.05	27.07	**1357.28**	**1355.90**	**19.56**	1361.69
r207	1268.66	**1256.22**	28.18	1364.12	1359.76	**23.60**	**1260.31**	1257.88	24.61	1256.22
r208	1208.89	1198.39	29.02	1289.03	1281.92	34.43	**1198.80**	**1195.96**	**28.35**	1198.39
r209	1345.50	1333.33	30.30	1407.39	1381.34	25.18	**1329.72**	**1321.76**	**20.01**	1333.33
r210	1324.07	1314.16	30.07	1385.87	1359.10	25.44	**1301.00**	**1298.78**	**19.12**	1314.16
r211	1244.73	1231.38	26.30	1326.35	1319.15	**21.33**	**1233.22**	**1226.74**	23.49	1231.38
rc101	2560.33	2548.84	13.71	**2508.65**	2504.72	9.42	2514.33	**2501.78**	**8.63**	2504.72
rc102	2359.92	2330.50	14.35	2335.72	2334.08	9.68	**2326.17**	**2315.01**	**9.07**	2330.50
rc103	2136.78	**2105.84**	14.14	**2113.31**	2108.82	10.78	2126.76	2116.31	**9.79**	2105.84
rc104	2002.33	1986.35	15.56	1984.66	1979.16	14.39	**1980.44**	**1973.78**	**10.48**	1979.16
rc105	2287.95	2259.97	13.87	2264.49	2252.05	9.81	**2259.34**	**2250.37**	**9.18**	2252.05
rc106	2232.05	2209.73	14.50	**2194.98**	**2187.30**	10.21	2213.35	2194.61	**9.71**	2187.30
rc107	2050.20	2037.25	15.43	**2039.77**	2034.35	15.20	2043.64	**2012.53**	**9.69**	2034.35
rc108	1995.41	**1962.87**	14.99	1975.91	1969.75	16.03	**1974.87**	1967.99	**9.98**	1962.87
rc201	1931.42	**1899.99**	15.69	2013.94	1976.91	16.64	**1912.42**	**1899.99**	**10.71**	1899.99
rc202	1825.07	1807.30	16.19	1921.19	1876.72	19.55	**1807.50**	**1805.24**	**14.68**	1807.30
rc203	1660.93	1642.43	19.00	1749.83	1717.98	22.51	**1649.11**	**1637.32**	**15.48**	1642.43
rc204	1543.04	1521.80	22.13	1638.89	1597.07	34.12	**1526.04**	**1520.59**	**19.91**	1521.80
rc205	1774.22	1753.79	19.03	1892.25	1832.28	21.98	**1758.96**	**1747.39**	**13.08**	1753.79
rc206	1767.75	1751.75	17.79	1883.33	1819.18	23.71	**1757.36**	**1742.98**	**13.91**	1751.75
rc207	1640.23	1616.96	19.07	1782.89	1694.69	27.96	**1611.17**	**1603.23**	**15.34**	1616.96
rc208	1520.76	1497.95	22.03	1660.49	1578.86	32.61	**1499.75**	**1495.34**	**21.06**	1497.95
Avg			21.47			21.96			15.05	
Gap	1.23	0.22		2.33	1.52		0.29	-0.13		

Table A.2: Comparison with the best known solutions for the E-FSMFTW, Type-B. HPRH: Hiermann et al. (2016); Montoya (2016).

C		HPRH			Montoya			HGA		BKS
Name	Avg 10	Best 10	T(min)	Avg 10	Best 10	T(min)	Avg 10	Best 10	T(min)	
c101	1816.06	1810.12	14.08	1820.45	1810.12	8.84	**1809.97**	**1809.93**	**7.06**	1809.93*
c102	1766.14	**1759.73**	14.36	1770.44	1763.97	9.20	**1759.73**	**1759.73**	**7.91**	1759.73
c103	1759.20	1755.02	15.09	**1757.68**	1746.80	20.76	**1745.33**	**1744.92**	**11.06**	1746.80
c104	1735.86	1719.67	15.60	**1727.72**	1721.53	29.04	**1718.73**	**1717.33**	**10.10**	1719.67
c105	1785.43	**1783.25**	14.51	1790.59	1785.31	10.66	**1783.92**	**1783.25**	**7.19**	1783.25
c106	1777.67	1774.77	14.64	1780.39	1775.08	11.10	**1773.57**	**1772.74**	**8.09**	1774.77
c107	1768.33	**1764.02**	14.57	1775.74	1765.45	14.68	**1765.09**	**1764.02**	**7.90**	1764.02
c108	1769.76	1761.41	14.80	1772.78	1768.05	20.58	**1762.95**	**1760.63**	**8.79**	1761.41
c109	1749.07	1740.18	15.30	**1749.05**	1744.09	29.92	**1740.78**	**1738.93**	**9.17**	1740.18
c201	1213.63	1210.41	31.30	**1210.50**	**1210.41**	**13.50**	**1210.41**	**1210.41**	13.84	1210.41
c202	1220.97	**1209.73**	34.17	**1210.12**	**1209.73**	16.58	**1209.86**	**1209.73**	**15.72**	1209.73
c203	1227.69	1212.34	33.07	**1226.22**	1216.18	30.01	**1208.22**	**1207.95**	**17.96**	1212.34
c204	1199.37	1179.25	32.15	1232.00	1204.68	35.62	**1177.50**	**1175.94**	**20.00**	1179.25
c205	1195.24	1188.92	31.64	1195.35	1192.54	16.70	**1192.69**	**1188.92**	**15.94**	1188.92
c206	1192.30	**1183.42**	31.01	**1191.74**	1188.81	20.16	**1183.42**	**1183.42**	**17.40**	1183.42
c207	1190.37	**1183.42**	31.44	1190.65	1187.49	21.52	**1183.42**	**1183.42**	**17.17**	1183.42
c208	1192.96	**1181.47**	30.82	**1192.42**	1182.60	23.78	**1181.47**	**1181.47**	**16.70**	1181.47
r101	1977.89	1961.02	14.36	**1959.07**	1959.04	9.45	**1957.89**	1954.56	**7.82**	1954.00*
r102	1791.03	1765.36	14.67	**1767.00**	1761.48	**7.54**	**1760.92**	1757.91	8.64	1757.13*
r103	1618.81	1601.23	15.52	**1593.13**	**1587.32**	12.54	1603.05	1589.17	**9.65**	1587.32
r104	1448.31	1424.30	16.20	**1437.37**	1427.76	19.66	**1435.56**	**1417.69**	**10.97**	1424.30
r105	1728.12	1704.36	14.68	**1705.56**	**1699.34**	**8.25**	1714.26	1708.92	9.10	1699.34*
r106	1635.42	1611.62	14.67	**1612.20**	1609.78	**8.55**	1623.31	**1603.24**	9.55	1604.55
r107	1514.01	**1490.04**	15.99	**1499.00**	1493.12	17.35	1500.84	1493.27	**10.27**	1490.04
r108	1417.39	1399.27	16.42	**1404.05**	1397.86	18.13	**1399.22**	**1389.46**	**10.58**	1397.86
r109	1580.14	1560.34	15.65	**1554.22**	1551.69	16.98	1566.61	1552.48	**10.03**	1550.40
r110	1471.66	1446.48	15.64	**1429.38**	**1420.13**	12.11	1447.59	1434.84	**10.43**	1420.13
r111	1479.75	1457.68	16.16	**1443.94**	1439.02	12.62	1460.14	1441.99	**10.53**	1438.81
r112	1403.82	1389.87	16.10	**1394.19**	1388.22	25.74	1398.31	**1385.84**	**10.98**	1388.22
r201	1378.77	**1366.63**	29.69	1480.55	1474.75	39.50	**1378.37**	1368.94	**13.30**	1366.63
r202	1249.65	**1236.97**	29.13	1328.35	1316.45	42.06	**1249.56**	1245.49	**17.10**	1236.97
r203	1124.07	1104.85	30.23	1205.32	1183.71	56.20	**1107.65**	**1102.56**	**19.49**	1104.85
r204	983.97	**977.72**	26.81	1050.51	1032.48	65.96	**978.93**	**977.72**	**24.84**	977.72
r205	1232.63	1217.77	29.15	1308.90	1293.54	47.77	**1205.62**	**1197.20**	**17.35**	1217.77
r206	1155.47	1136.83	30.95	1239.18	1230.67	60.69	**1133.39**	**1130.90**	**18.26**	1136.83
r207	1057.22	**1031.22**	26.31	1136.77	1110.93	58.58	**1033.95**	**1031.22**	**23.80**	1031.22
r208	984.87	971.15	28.21	1049.20	1032.20	85.72	**973.34**	**970.96**	**28.08**	971.15
r209	1117.68	1099.24	29.62	1170.58	1156.34	57.01	**1100.36**	**1092.26**	**18.11**	1099.24
r210	1100.27	1087.21	29.88	1143.99	1134.10	57.33	**1077.86**	**1069.71**	**18.35**	1087.21
r211	1026.07	1006.38	25.93	1098.37	1087.95	51.81	**1005.16**	**1001.74**	**22.23**	1006.38
rc101	2153.24	2142.24	13.80	**2123.26**	2121.02	**8.96**	2134.84	**2119.70**	**8.96**	2121.02
rc102	1972.85	1957.11	14.68	**1950.16**	1947.54	**9.40**	1959.96	**1945.31**	9.60	1947.54
rc103	1764.22	1736.25	14.54	**1736.49**	**1726.85**	10.72	1745.83	1733.70	**10.03**	1726.85
rc104	1614.09	1595.44	15.80	**1605.91**	1596.18	15.20	**1596.48**	**1584.79**	**10.40**	1595.44
rc105	1900.42	1885.63	14.14	**1880.03**	1875.91	9.93	1881.65	**1870.80**	**9.67**	1875.91
rc106	1844.99	1823.89	15.18	**1814.49**	1811.86	9.96	**1814.28**	**1808.96**	**9.90**	1811.86
rc107	1675.58	1639.84	15.31	**1659.27**	1645.79	15.60	**1656.95**	**1635.51**	**10.19**	1639.84
rc108	1601.47	**1578.51**	14.98	**1588.87**	1583.70	14.15	**1586.20**	1583.08	**10.91**	1578.51
rc201	1617.52	1589.99	15.64	1682.78	1664.90	14.79	**1598.69**	**1588.25**	**11.07**	1589.99
rc202	1497.99	1485.13	16.72	1587.09	1541.00	**15.11**	**1483.05**	**1481.05**	15.40	1485.13
rc203	1333.25	**1310.37**	19.35	1363.51	1345.08	48.90	**1316.19**	1310.48	**16.57**	1310.37
rc204	1193.93	1183.16	22.69	1224.22	1212.07	77.59	**1186.42**	**1182.32**	**21.22**	1183.16
rc205	1440.00	1424.75	20.95	1508.13	1500.24	39.75	**1426.02**	**1422.39**	**14.55**	1424.75
rc206	1439.17	1431.21	18.11	1493.94	1473.86	43.46	**1434.12**	**1429.47**	**14.54**	1431.21
rc207	1299.14	1277.71	21.30	1364.75	1344.75	49.95	**1280.53**	**1273.23**	**15.47**	1277.71
rc208	1171.52	1161.57	22.91	1216.16	1202.33	64.83	**1163.21**	**1159.70**	**22.02**	1161.57
Avg			20.83			28.08			13.61	
Gap	1.27	0.21		2.31	1.64		0.33	-0.10		

Table A.3: Comparison with the best known solutions for the E-FSMFTW, Type-C. HPRH: Hiermann et al. (2016); Montoya (2016).